

UCSF

UC San Francisco Electronic Theses and Dissertations

Title

The Decoy Receptor IL-1R2 Attenuates Treg Activation in Tumors

Permalink

<https://escholarship.org/uc/item/5qm8z8gf>

Author

Habrylo, Ireneusz

Publication Date

2023

Peer reviewed|Thesis/dissertation

The Decoy Receptor IL-1R2 Attenuates Treg Activation in Tumors

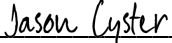
by
Ireneusz Bartłomiej Habryło

DISSERTATION
Submitted in partial satisfaction of the requirements for degree of
DOCTOR OF PHILOSOPHY

in
Biomedical Sciences

in the
GRADUATE DIVISION
of the
UNIVERSITY OF CALIFORNIA, SAN FRANCISCO

Approved:


DocuSigned by:

5FFFC327038A40D... Jason Cyster
Chair

DocuSigned by:

DocuSigned by: 0364EC... Ari Molofsky

DocuSigned by:

DocuSigned by: 04BA... Qizhi Tang

DocuSigned by:

B9C7E7603EE44D5... Michael Rosenblum

Committee Members

Copyright 2023

By

Ireneusz Bartłomiej Habryło

Acknowledgements

Chapter 1 of this dissertation contains text adapted from **Gouirand V, Habrylo I, and Rosenblum MD. Regulatory T Cells and Inflammatory Mediators in Autoimmune Disease. *Journal of Investigative Dermatology* (2022).** The included sections were primarily written by the author (Habrylo I), with editing and feedback from the listed co-authors. Rosenblum MD directed and supervised the research that forms the basis for this chapter.

Chapter 2 of this dissertation is a reprint of **Habrylo et al. IL-1R2 Attenuates Regulatory T cell Activation in Tumors. *Submitted* (2023).** Rosenblum MD supervised the research that forms the basis for this chapter. Cohen JN, Marathe S, Macon CE, Moss M, Lowe MM, Moreau JM, Mahuron KM, Daud AI, Pauli ML, Barbee SD, Kleinschek MA, and Yohn CB assisted with data collection and analysis.

Contributions

Gouirand V*, Habrylo I*, Rosenblum MD. **Regulatory T Cells and Inflammatory Mediators in Autoimmune Disease.** *J Invest Dermatol.* 2022 Mar;142(3 Pt B):774-780. doi: 10.1016/j.jid.2021.05.010. Epub 2021 Jul 18. *Authors contributed equally.

Habrylo I, Cohen JN, Marathe S, Macon CE, Moss MI, Lowe MM, Moreau JM, Mahuron KM, Daud AI, Pauli ML, Barbee SD, Kleinschek MA, Yohn CB, Rosenblum MD. **IL-1R2 Attenuates Regulatory T cell Activation in Tumors.** 2023. *Submitted.*

Remember, upon the conduct of each depends the fate of all.

— Alexander the Great

Abstract

The Decoy Receptor, IL-1R2, Attenuates Treg Activation in Tumors

Ireneusz Bartłomiej Habryło

Interleukin-1 (IL-1) is a pleiotropic cytokine with complex biology. Because of its potent pro-inflammatory properties, several mechanisms have evolved to regulate its systemic and local effects. At the tissue level, a non-signaling decoy receptor, Interleukin-1 receptor 2 (IL-1R2) plays a major role in attenuating IL-1 mediated signaling. IL-1R2 is highly expressed on regulatory T cells (Tregs) that infiltrate both mouse and human tumors. Tregs respond to cytokines in their local environment to modulate their activity. IL-1 signaling is thought to regulate Treg effector function in the context of Type 1 and Type 17 inflammation and has primarily been characterized in autoimmune diseases. However, the function of IL-1 in tumor Treg biology is relatively unknown. Here, we show that a subset of highly activated Tregs induce IL-1R2 expression upon migration into tumors. In contrast to myeloid cells, induction of IL-1R2 on Tregs was mediated by T cell receptor (TCR) engagement and not IL-1-mediated signaling. Signaling through the canonical IL-1 receptor (IL-1R1) activated Tregs to express a unique gene expression signature and IL-1R2 potently attenuated this activation module in tumors. Accordingly, deletion of IL-1R2 on Tregs resulted in a more suppressive tumor microenvironment and increased tumor growth. In translational studies, we developed a novel IL-1R2 depleting antibody which was highly selective for tumor infiltrating Tregs. Tumor Treg depletion using this approach potently inhibited tumor growth without generating systemic autoimmunity. Taken together, we define the biology of IL-1R2 expression on tumor Tregs and provide the foundation for a novel therapeutic strategy to augment anti-tumor immunity.

Table of Contents

CHAPTER 1: Inflammatory mediators in regulatory T cell function	1
1.1 Treg heterogeneity and effector functions.....	1
1.2 Tregs and Type 1 immunity.....	3
1.3 Tregs and Type 17 immunity.....	5
1.4 Discussion.....	8
1.5 References.....	11
1.6 Figure.....	19
CHAPTER 2: Decoy receptor IL-1R2 in tumor-associated Treg biology	20
2.1 Introduction.....	20
2.2 Suppressive Tregs highly express IL-1R2 in human tumors.....	22
2.3 IL-1R2 ⁺ tumor Tregs are not predominantly derived from adjacent skin.....	24
2.4 Tumor Tregs upregulate IL-1R2 in response to TCR stimulation but not IL-1 family members.....	25
2.5 IL-1R2 expression on Tregs results in reduced tumor growth <i>in vivo</i>	27
2.6 IL-1R2 attenuates Treg activation in tumors.....	29
2.7 Depleting IL-1R2 expressing Tregs reduces tumor growth.....	31
2.8 Discussion.....	33
2.9 Methods.....	38
2.10 References.....	48
2.11 Figures.....	61

List of Figures

Figure 1.1 Mechanisms of regulatory T cell (Treg) suppression.....	19
Figure 2.1 Regulation of interleukin-1 (IL-1) signaling.....	61
Figure 2.2 Suppressive Tregs highly express IL-1R2 in human tumors.....	62
Figure 2.3 IL-R2 ⁺ tumor Tregs are not predominantly derived from adjacent skin.....	64
Figure 2.4 Tumor Tregs upregulate IL-1R2 in response to TCR stimulation but not IL-1 family members.....	65
Figure 2.5 IL-1R2 expression on Tregs results in reduced tumor growth <i>in vivo</i>	67
Figure 2.6 IL-1R2 attenuates Treg activation in tumors.....	69
Figure 2.7 Depleting IL-1R2 expressing Tregs reduces tumor growth.....	71
Figure 2.8 Model of IL-1R2 function on tumor Tregs.....	72
Figure 2.9 Supplement to suppressive Tregs highly express IL-1R2 in human tumors.....	73
Figure 2.10 Il1r2-EGFP expression in tumor and skin of MC38-bearing mice.....	74
Figure 2.11 Supplement to tumor Tregs upregulate IL-1R2 in response to TCR stimulation but not IL-1 family members.....	75
Figure 2.12 Supplement to IL-1R2 expression on Tregs results in reduced tumor growth <i>in vivo</i>	76
Figure 2.13 Supplement to IL-1R2 attenuates Treg activation in tumors.....	77
Figure 2.14 Supplement to depleting IL-1R2 expressing Tregs reduces tumor growth.....	78

CHAPTER 1: Inflammatory mediators in regulatory T cell function

1.1 Treg heterogeneity and effector functions

Regulatory T cells primarily develop and differentiate in the thymus (tTregs). tTregs constitutively express the transcription factor Foxp3, possess a T cell receptor (TCR) of high affinity for ‘self’ and are the dominant mediators of peripheral tolerance to autoantigens¹. Alternatively, Tregs can be generated from naive CD4⁺ T cells in the periphery (pTregs) in specific contexts. Resting CD4⁺ T cells exposed to IL-2 and TGF- β *ex vivo* begin to express Foxp3 and acquire many phenotypical and functional aspects of tTregs^{2,3}. Foxp3 controls the Treg transcriptional program and is essential for their immunoregulatory function at baseline and after activation⁴. Loss-of-function mutations in the *Foxp3* gene lead to severe autoimmunity, as illustrated by scurfy mice and IPEX syndrome in humans^{5,6}.

Regulatory T cells are a heterogeneous population comprised of multiple cell states and differentiated cell fates that differ with respect to their regulatory capacity and tissue-specific functions⁷. Major subsets of Tregs have been defined as: a) naïve or resting Tregs; b) activated or effector Tregs; c) memory Tregs; and d) T helper- (Th-) like Tregs. These cell states reflect a Treg’s present environment, including exposure to antigen and inflammatory mediators, i.e., cytokines, along with their history of exposures. CD25^{low} Tregs can reduce Foxp3 expression and be skewed toward a Th-like lineage through similar cytokine signals that polarize T helper cells⁸. Tregs driven towards Th differentiation in this fashion express many components of the transcriptional machinery that mirrors their Th counterparts but fail to secrete high levels of Th-associated cytokines. This differentiation allows Th1- and Th17-like Tregs to optimally regulate Th1 and Th17 cells, respectively⁹. Similarly, Th2-like Tregs regulate Th2 cells in allergy and

autoimmunity but are not discussed in this work. These type-2 cells do not depend on interleukin-1 (IL-1) signaling, and have not been described in tumor biology.

The role of cytokines on Treg function has primarily been studied in the context of autoimmunity and tissue inflammation. Autoimmune diseases are thought to result from an imbalance between the relative abundance and activation of pro-inflammatory cells and regulatory cells. Proportional reductions in the number and function of Tregs are thought to be key contributors to the development and maintenance of tissue inflammation. For example, specific autoimmune diseases are characterized by a decreased ratio of Tregs to effector Th (Teff) cells, such as a low Treg:Th17 ratios¹⁰⁻¹² and a reduction of their suppressive activity¹³⁻¹⁶. The opposite phenomenon is observed in tumors, where Treg suppression hinders tumor immune rejection, and low Treg:CD8⁺ T cell ratios are associated with improved patient outcomes^{17,18}. As in inflamed tissue, tumor Tregs are exposed to a variety of cytokines and chemokines released by injured cells, other immune cells, and potentially the tumor itself¹⁹. Tregs integrate these signals and modulate their suppression in response.

Tregs suppress innate and adaptive immunity through a variety of mechanisms (**Figure 1.1**). These include but are not limited to: (1) starving T cells of IL-2, (2) promoting T cell apoptosis, (3) modulating T cell metabolism to reduce effector function, (4) secreting anti-inflammatory cytokines; and (5) inhibiting immunostimulatory signals on antigen presenting cells (APCs)⁷. While these canonical mechanisms of Treg suppression are broadly applicable, advances in mouse models and targeted antibody therapy in humans have revealed disease- and tissue-specific signaling pathways by which Tregs can modulate inflammation. We now appreciate that the local cytokine environment can influence Treg programming and function in tissues. Herein, we attempt to address the complex picture emerging whereby Tregs maintain a

delicate balance of differentiating towards the cell types they need to most optimally suppress and adopting pro-inflammatory traits characteristic of these cells. A disruption in this balance has been proposed as an underlying mechanism contributing to chronic tissue inflammation.

1.2 Tregs and Type 1 immunity

Human and mouse Tregs can differentiate into Th1-like cells following excessive activation or exposure to type-1 inflammation. These Treg-Th1 cells can be induced to produce IFN γ and lose their suppressive function. Naïve CD4⁺ T cells can be converted to Th1 cells through IFN γ and IL-12 treatment *in vitro*, and this differentiation is dependent on the transcription factor *Tbx21* or T-bet²⁰. Alternatively, IL-1 β , IL-23, and IL-12 treatment can convert naïve cells or Th17s to a non-classical Th1 cell, which expresses CD161 and the IL-1 receptor, IL-1R1²¹. A subset of human Tregs will downregulate Foxp3 and express T-bet and IFN γ following extensive TCR activation²².

Treg-Th1 differentiation is highly dependent on IL-12, a pro-inflammatory cytokine known to enhance IFN γ production²³. IL-12 is associated with autoimmune diseases such as primary biliary cholangitis and Sjogren's syndrome. In both conditions, low dose administration of IL-12 results in an acquired Th1-like phenotype by Tregs *via* signal transducer and activator of transcription (STAT) 4 phosphorylation²⁴. IFN γ can induce Treg-Th1 cells directly *in vivo*²⁵. IFN γ plays a role in cell-mediated immune responses against viral infections, but excessive cytokine levels are associated with inflammatory and autoimmune diseases. Patients with autoimmune hepatitis, Sjogren's syndrome, and multiple sclerosis have IFN γ -secreting Tregs present at a relatively increased frequency in their peripheral blood²⁶⁻²⁸.

Treg-Th1 cells that express T-bet but not IFN γ are adapted to suppress Th1 cells in disease. T-bet induces expression of CXCR3, a chemokine receptor used by Th1 cells when migrating to inflamed tissue²⁹. Treg-Th1 cells also express CXCR3, allowing them to traffic to the site of Th1-mediated inflammation and suppress these cells. Mice treated with anti-CD40 antibody develop robust type 1 inflammation, associated with increased T-bet⁺ CXCR3⁺ Tregs³⁰. These Tregs can inhibit naïve T cell proliferation *in vitro*, indicating their suppressive function is preserved. T-bet may also be involved in Treg-Th1 homeostasis. In a mixed bone marrow chimera, T-bet-deficient Tregs were outcompeted by wild-type Tregs in the spleen following anti-CD40 treatment²⁹.

Tregs can become destabilized to lose suppressive capacity and begin producing IFN γ . These “ex-Tregs” downregulate Foxp3 and may promote autoimmune disease in humans³¹. IFN γ ⁺ Tregs extracted from patients with relapsing-remitting multiple sclerosis showed less suppressive capacity *in vitro*, which was partially reversed with anti-IFN γ treatment²³. Similarly, reduced suppression is observed in IFN γ ⁺ Tregs isolated from Type 1 diabetes patients³². In mice, IFN γ ⁺ Tregs may retain regulatory function in certain conditions. In a mouse model of colitis, a subset of intestinal Tregs began expressing IL-17A (Treg-Th17), while others began expressing IFN γ (Treg-Th1). The IFN γ ⁺ Tregs were able to suppress naïve T cell proliferation *in vitro*³³.

While IFN γ is generally thought to be pro-inflammatory, this cytokine may limit inflammation through direct effects on Tregs and indirect effects on other effector T cells. In mice, IFN γ neutralization and genetic deletion both abrogate Treg function³⁴. Interestingly, IFN γ may promote Treg generation, potentially through upregulating CD25 expression^{35,36}. IFN γ uses STAT1 as a signaling mediator. Though STAT1 has been identified as a powerful inhibitor of

Treg development in the periphery³⁷, the absence of STAT1 contributes to impaired development of Tregs and increases the risk of developing autoimmune disease³⁸. This cytokine also limits proliferation of some T cell subsets and induces apoptosis of naïve T cells and Th2 cells^{39,40}. In the experimental autoimmune encephalomyelitis (EAE) model of brain inflammation, MIS416 (a microparticle that activates NOD-2 and TLR-9-signaling) enhanced Treg function and proliferation in an IFN γ -dependent manner⁴¹. Rheumatoid arthritis patients treated with anti-TNF α (adalimumab) showed elevated IFN γ production by NK cells and an expansion of Tregs⁴².

Autoimmune disease therapies that target type-1 inflammation may also affect Treg-Th1 cells. Understanding and avoiding these unintended effects may improve disease outcomes, as Treg-Th1 cells optimally limit Th1- and Th17-mediated inflammation. Over the last decade, two clinical trials have investigated the potential of anti-IFN γ therapy for autoimmune disease treatment. Fontolizumab and AMG 811, two monoclonal antibodies against IFN γ , were tested in Crohn's disease⁴³ and RA in one trial arm, and lupus nephritis⁴⁴ in the other arm. Unfortunately, both trials failed to show a discernible clinical effect., This is most likely secondary to the complex biology of IFN γ in potentiating both pro-inflammatory and regulatory responses.

1.3 Tregs and Type 17 immunity

Th17 cells and Tregs use shared signals to induce their initial differentiation, and under the appropriate circumstances, Tregs can take on the transcriptional profile or cytokine production of Th17 cells to form Treg-Th17 cells. Naïve CD4⁺ T cells can be skewed toward a Th17 lineage via addition of TGF- β and IL-6 *in vitro*, and this polarization is dependent on the transcription factor STAT3⁴⁵. The addition of IL-23 can further induce a pathogenic Th17 phenotype with increased secretion of inflammatory cytokines. Tregs secrete and activate latent

TGF- β , and TGF- β without IL-6 skews CD4 cells toward an induced Treg lineage, highlighting the interconnectedness of these two cell types⁴⁶. IL-1 β and IL-6 treatment can induce ROR γ t and IL-17A expression in human Tregs, while retaining suppressive function in most circumstances^{47,48}.

IL-17A is required for mucosal immunity against extracellular pathogens, but also plays a role in autoimmune inflammation⁴⁹. IL-17A induces production of antimicrobial peptides and granulocyte colony-stimulating factor (G-CSF) to mobilize neutrophils to the site of infection⁵⁰. Excessive IL-17 signaling contributes to several autoimmune conditions, including psoriasis, psoriatic arthritis, and ankylosing spondylitis. Th17 cells express IL-21 in severe psoriasis, which promotes upregulation of ROR γ t and suppression of Foxp3 in Tregs⁵¹. A low Treg/Th17 ratio has been implicated in inflammatory bowel disease (IBD), systemic lupus erythematosus (SLE), multiple sclerosis (MS), and autoimmune hepatitis⁵²⁻⁵⁴. Given the plasticity between Tregs and Th17 cells, this simple metric may overlook intermediate cell types with either suppressive or inflammatory function.

When exposed to type-17 cytokines, mouse and human Tregs can upregulate Th17 transcription factors without production of IL-17A. These Treg-Th17 cells retain their suppressive function and are better adapted to block Th17 cell mediated inflammation. In mouse models of colitis, Treg suppression is dependent on STAT3, suggesting that Tregs co-opt a type 17 transcriptional program to better regulate pathogenic Th17 cells⁵⁵. STAT3-deficient Tregs can suppress T cell proliferation *in vitro* but are unable to suppress Th17 differentiation in colitis and mice develop fatal intestinal inflammation. Treg-Th17 cells may be optimized to suppress Th17 cells due to their localization. In a pristane-induced model of lupus (SLE), Treg17 cells limited Th17-mediated peritoneal and renal inflammation. Treg-Th17 cells in these tissues expressed the

chemokine receptor CCR6, which activated Th17 cells utilize to traffic to sites of inflammation. STAT3-deficient Tregs showed reduced CCR6 expression and reduced migration to inflamed tissue⁵⁶. In human Treg cultures, ROR γ ⁺ Treg-Th17 cells can also be identified by CCR6 expression⁵⁷.

Treg17 cells can release pro-inflammatory IL-17A while maintaining suppressive function. IL-17A production by human Tregs is enhanced by IL-1 β , IL-23, and IL-21 treatment *in vitro*, and the process is partly dependent on epigenetic modifications. Inhibition of histone deacetylase (HDAC) activity reduced IL-17 production in human Tregs⁵⁷. These IL-17-secreting Treg-Th17 cells retain suppressive function in response to weak TCR stimulation, but transiently lose their regulatory function in response to strong TCR and APC stimulation⁴⁷. This mechanism may be mediated *via* tumor-necrosis factor receptor super family (TNFRSF) signaling on Tregs. In mice, TNFR receptors prevent them from expressing ROR γ t and IL-17A under healthy conditions. Defects in both CD27 (TNFRSF7) and OX40 (TNFRSF4) cause Tregs to express high levels of IL-17A and lose suppressive function in mouse models of skin inflammation⁵⁸. This temporary and rapid switch between regulatory or effector function could allow Tregs to precisely modulate the amount of tissue inflammation in a rapid manner. Treg-Th17 cells could therefore be adapted to maintain a set level of inflammation in auto-immune disease or cancer, but the effect of these cells on human disease is unclear.

IL-17A-producing Treg-Th17 cells have been identified in human autoimmune disease, but the clinical implications of these cells is unclear. Treg-Th17 cells have been described in psoriasis, hidradenitis suppurativa, systemic sclerosis, and autoimmune hepatitis^{53,59-61}. In psoriasis patients, lesion severity is associated with Treg-Th17 levels, but it is unclear if the Treg-Th17 cells are contributing or merely following inflammation. In systemic sclerosis, IL-

17A-expressing Tregs had reduced suppressive capacity and CTLA-4 expression, suggesting that Treg-Th17 cells may be pathogenic in these patients.

Therapies that target Th17 cells in autoimmune disease may also alter Treg-Th17 cells. In autoimmune hepatitis patients, blocking IL-17 signaling by several methods increased Foxp3 expression on Tregs and their suppressive capacity. Similarly, inhibiting IL-1 signaling may reduce Treg differentiation toward a pro-inflammatory state. In human rheumatoid arthritis patients, recombinant IL-1 receptor antagonist (hIL-1Ra) treatment decreased IL-17 expression on Tregs in peripheral blood and increased Foxp3 expression. In mice, the same hIL-1Ra treatment induced Treg differentiation in the spleen⁶². IL-17 and IL-1 modulating therapies are already used to treat autoimmune disease, and part of their effect may be mediated through inhibition of abnormally functioning pathogenic Treg-Th17 cells. As some of these cells still maintain suppressive function, it will be important to mechanistically delineate between healthy and pathogenic Treg-Th17 cells in the hopes of developing novel therapies that skew towards the more suppressive or 'regulatory' state in autoimmune disease or less suppressive in cancer.

1.4 Discussion

Tregs were initially described as a relatively homogeneous cell population. However, we now appreciate that these cells can have varied origins, localization, and function. In addition, these cells, and their CD4⁺ Teff counterparts, demonstrate plasticity, altering their phenotype and function in response to the local cytokine milieu. Tregs have multiple effector programs that are based on the expression of master transcription factors in addition to Foxp3. These cells have co-opted the transcriptional regulators and programming of their Teff targets to better colocalize and

suppress these cells. Tregs will express T-bet, IRF4, and ROR γ t to inhibit Th1, Th2, and Th17 responses, respectively⁶³.

Tregs can adapt to their local environment through sensing of chemokines and cytokines. Tregs express the cytokine receptors for Th1- and Th17-polarizing cytokines. Under certain contexts, such as in inflamed tissue, Tregs can express the cytokines of their target cells, such as Treg-Th1s, which produce IFN γ and become pro-inflammatory cells or Treg-Th17s, which begin producing IL-17A but retain their suppressive capacity apart from excess. While Th2 differentiation is generally anti-inflammatory, it can mediate inflammation in certain autoimmune diseases. Treg-Th2 cells generally maintain suppressive capacity, but IL-4 and IL-13 released by these cells can still promote inflammation. In practice, these relationships are complicated by multiple functions of each cytokine.

A better understanding of how Tregs sense and respond to their local cytokine environment is critical in our attempt to elucidate how these cells function in healthy tissues and the mechanisms by which dysfunctional Tregs may contribute to autoimmune disease or tumor immune suppression. While a greater ratio or frequency of Tregs is generally considered to better control tissue inflammation, understanding the expression profile and heterogeneity of these cells is extremely important. An expansion of Tregs that have lost suppressive capacity in favor of pro-inflammatory cytokine production may not be clinically efficacious.

As new antibody and small molecule therapies continue to be developed for autoimmune diseases, it is important to be aware of how these might affect Tregs with different effector functions. Similarly, when designing therapies to expand Treg populations either *in vivo* or *ex vivo*, targeting an appropriately polarized subset of Tregs for expansion may be more efficient and effective to suppress the relevant form of inflammation⁶⁴. Conversely, Treg depletion

approaches are being explored to bolster anti-tumor immunity⁶⁵. Surface markers preferentially expressed on tumor-infiltrating but not circulating Tregs are desirable targets for depleting approaches, and many of these are receptors for inflammatory cytokines, including TNF α and IL-1. But due to the conserved nature of biology, these cytokine receptors can be located on a broad range of cell types. Understanding the local inflammatory environment and how Tregs respond to these cytokines is critical for the development of new Treg depletion therapies.

1.5 References

1. Sakaguchi, S., Yamaguchi, T., Nomura, T. & Ono, M. Regulatory T Cells and Immune Tolerance. *Cell* vol. 133 775–787 (2008).
2. Zheng, S. G., Wang, J., Wang, P., Gray, J. D. & Horwitz, D. A. IL-2 Is Essential for TGF- β to Convert Naive CD4 + CD25 – Cells to CD25 + Foxp3 + Regulatory T Cells and for Expansion of These Cells. *The Journal of Immunology* **178**, 2018–2027 (2007).
3. Chen, W. J. *et al.* Conversion of Peripheral CD4+CD25- Naive T Cells to CD4+CD25+ Regulatory T Cells by TGF- β Induction of Transcription Factor Foxp3. *Journal of Experimental Medicine* **198**, 1875–1886 (2003).
4. Hori, S., Nomura, T. & Sakaguchi, S. Control of regulatory T cell development by the transcription factor Foxp3. *Journal of Immunology* **198**, 981–985 (2003).
5. Brunkow, M. E. *et al.* Disruption of a new forkhead/winged-helix protein, scurfy, results in the fatal lymphoproliferative disorder of the scurfy mouse. *Nat Genet* **27**, 68–73 (2001).
6. Bennett, C. L. *et al.* The immune dysregulation, polyendocrinopathy, enteropathy, X-linked syndrome (IPEX) is caused by mutations of FOXP3. *Nat Genet* **27**, 20–21 (2001).
7. Shevyrev, D. & Tereshchenko, V. Treg Heterogeneity, Function, and Homeostasis. *Frontiers in Immunology* vol. 10 3100 (2020).
8. Komatsu, N. *et al.* Pathogenic conversion of Foxp3 + T cells into TH17 cells in autoimmune arthritis. *Nat Med* **20**, 62–68 (2014).

9. Duhon, T., Duhon, R., Lanzavecchia, A., Sallusto, F. & Campbell, D. J. Functionally distinct subsets of human FOXP3 + Treg cells that phenotypically mirror effector Th cells. *Blood* **119**, 4430–4440 (2012).
10. Wang, W. *et al.* The Th17/Treg imbalance and cytokine environment in peripheral blood of patients with rheumatoid arthritis. *Rheumatol Int* **32**, 887–893 (2012).
11. Lee, G. R. The balance of th17 versus treg cells in autoimmunity. *International Journal of Molecular Sciences* vol. 19 (2018).
12. Niu, Q., Cai, B., Huang, Z. C., Wang, L. I. & Shi, Y. Y. Disturbed Th17/Treg balance in patients with rheumatoid arthritis. *Rheumatol Int* **32**, 2731–2736 (2012).
13. Lawson, C. A. *et al.* Early rheumatoid arthritis is associated with a deficit in the CD4+CD25high regulatory T cell population in peripheral blood. *Rheumatology* **45**, 1210–1217 (2006).
14. Viglietta, V., Baecher-Allan, C., Weiner, H. L. & Hafler, D. A. Loss of Functional Suppression by CD4+CD25+ Regulatory T Cells in Patients with Multiple Sclerosis. *Journal of Experimental Medicine* **199**, 971–979 (2004).
15. Venken, K. *et al.* Compromised CD4⁺ CD25^{high} regulatory T-cell function in patients with relapsing-remitting multiple sclerosis is correlated with a reduced frequency of FOXP3-positive cells and reduced FOXP3 expression at the single-cell level. *Immunology* **123**, 79–89 (2008).
16. Ehrenstein, M. R. *et al.* Compromised function of regulatory T cells in rheumatoid arthritis and reversal by anti-TNF α therapy. *Journal of Experimental Medicine* **200**, 277–285 (2004).

17. Sato, E. *et al.* Intraepithelial CD8⁺ tumor-infiltrating lymphocytes and a high CD8⁺/regulatory T cell ratio are associated with favorable prognosis in ovarian cancer. *Proc Natl Acad Sci U S A* **102**, 18538–18543 (2005).
18. Baras, A. S. *et al.* The ratio of CD8 to Treg tumor-infiltrating lymphocytes is associated with response to cisplatin-based neoadjuvant chemotherapy in patients with muscle invasive urothelial carcinoma of the bladder. *Oncoimmunology* **5**, (2016).
19. Dranoff, G. Cytokines in cancer pathogenesis and cancer therapy. *Nature Reviews Cancer* 2004 4:1 **4**, 11–22 (2004).
20. Wilson, C. B., Rowell, E. & Sekimata, M. Epigenetic control of T-helper-cell differentiation. *Nature Reviews Immunology* vol. 9 91–105 (2009).
21. Santarlasci, V., Cosmi, L., Maggi, L., Liotta, F. & Annunziato, F. IL-1 and T helper immune responses. *Frontiers in Immunology* vol. 4 (2013).
22. Hoffmann, P. *et al.* Loss of FOXP3 expression in natural human CD4⁺ CD25⁺ regulatory T cells upon repetitive *in vitro* stimulation. *Eur J Immunol* **39**, 1088–1097 (2009).
23. Dominguez-Villar, M., Baecher-Allan, C. M. & Hafler, D. A. Identification of T helper type 1-like, Foxp3⁺ regulatory T cells in human autoimmune disease. *Nat Med* **17**, (2011).
24. Liaskou, E. *et al.* Increased sensitivity of Treg cells from patients with PBC to low dose IL-12 drives their differentiation into IFN- γ secreting cells. *J Autoimmun* **94**, 143–155 (2018).
25. Zagorulya, M. *et al.* Tissue-specific abundance of interferon-gamma drives regulatory T cells to restrain DC1-mediated priming of cytotoxic T cells against lung cancer. *Immunity* **56**, 386-405.e10 (2023).

26. Yamada, A. *et al.* Impaired expansion of regulatory T cells in a neonatal thymectomy-induced autoimmune mouse model. *American Journal of Pathology* **185**, 2886–2897 (2015).
27. Kitz, A. *et al.* AKT isoforms modulate Th1-like Treg generation and function in human autoimmune disease. *EMBO Rep* **17**, 1169–1183 (2016).
28. Arterbery, A. S. *et al.* Production of Proinflammatory Cytokines by Monocytes in Liver-Transplanted Recipients with De Novo Autoimmune Hepatitis Is Enhanced and Induces T H 1-like Regulatory T Cells. *The Journal of Immunology* **196**, 4040–4051 (2016).
29. Koch, M. A. *et al.* The transcription factor T-bet controls regulatory T cell homeostasis and function during type 1 inflammation. *Nat Immunol* **10**, 595–602 (2009).
30. Ferlin, W. G. *et al.* The induction of a protective response in *Leishmania major*-infected BALB/c mice with anti-CD40 mAb. *Eur J Immunol* **28**, 525–531 (1998).
31. McClymont, S. A. *et al.* Plasticity of Human Regulatory T Cells in Healthy Subjects and Patients with Type 1 Diabetes. *The Journal of Immunology* **186**, 3918–3926 (2011).
32. Feng, T., Cao, A. T., Weaver, C. T., Elson, C. O. & Cong, Y. Interleukin-12 converts Foxp3⁺ regulatory T cells to interferon- γ -producing Foxp3⁺ T cells that inhibit colitis. *Gastroenterology* **140**, 2031–2043 (2011).
33. Sawitzki, B. *et al.* IFN- γ production by alloantigen-reactive regulatory T cells is important for their regulatory function in vivo. *Journal of Experimental Medicine* **201**, 1925–1935 (2005).

34. Johnson-Huang, L. M. *et al.* Post-therapeutic relapse of psoriasis after CD11a blockade is associated with T cells and inflammatory myeloid DCs. *PLoS One* **7**, (2012).
35. Wang, Z. *et al.* Role of IFN- γ in induction of Foxp3 and conversion of CD4⁺CD25⁻ T cells to CD4⁺ Tregs. *Journal of Clinical Investigation* **116**, 2434–2441 (2006).
36. Caretto, D., Katzman, S. D., Villarino, A. V., Gallo, E. & Abbas, A. K. Cutting Edge: The Th1 Response Inhibits the Generation of Peripheral Regulatory T Cells. *The Journal of Immunology* **184**, 30–34 (2010).
37. Nishibori, T., Tanabe, Y., Su, L. & David, M. Impaired Development of CD4⁺ CD25⁺ Regulatory T Cells in the Absence of STAT1: Increased Susceptibility to Autoimmune Disease. *Journal of Experimental Medicine* **199**, 25–34 (2004).
38. Kishimoto, K. *et al.* Th1 cytokines, programmed cell death, and alloreactive T cell clone size in transplant tolerance. *Journal of Clinical Investigation* **109**, 1471–1479 (2002).
39. Martin, B. *et al.* Suppression of CD4⁺ T Lymphocyte Effector Functions by CD4⁺ CD25⁺ Cells In Vivo. *The Journal of Immunology* **172**, 3391–3398 (2004).
40. White, M. P. J., Webster, G., Leonard, F. & La Flamme, A. C. Innate IFN- γ ameliorates experimental autoimmune encephalomyelitis and promotes myeloid expansion and PDL-1 expression. *Sci Rep* **8**, (2018).
41. Aravena, O. *et al.* Anti-TNF therapy in patients with rheumatoid arthritis decreases Th1 and Th17 cell populations and expands IFN- γ -producing NK cell and regulatory T cell subsets. *Immunobiology* **216**, 1256–1263 (2011).

42. Reinisch, W. *et al.* Fontolizumab in moderate to severe Crohn's disease: A phase 2, randomized, double-blind, placebo-controlled, multiple-dose study. *Inflamm Bowel Dis* **16**, 233–242 (2010).
43. Boedigheimer, M. J. *et al.* Safety, pharmacokinetics and pharmacodynamics of AMG 811, an anti-interferon- γ monoclonal antibody, in SLE subjects without or with lupus nephritis. *Lupus Sci Med* **4**, e000226 (2017).
44. Miossec, P., Korn, T. & Kuchroo, V. K. Interleukin-17 and Type 17 Helper T Cells. *New England Journal of Medicine* **361**, 888–898 (2009).
45. Bettelli, E. *et al.* Reciprocal developmental pathways for the generation of pathogenic effector TH17 and regulatory T cells. *Nature* **441**, 235–238 (2006).
46. Beriou, G. *et al.* IL-17-producing human peripheral regulatory T cells retain suppressive function. *Blood* **113**, 4240–4249 (2009).
47. Kleinewietfeld, M. & Hafler, D. A. *The plasticity of human Treg and Th17 cells and its role in autoimmunity. Seminars in Immunology* vol. 25 305–312 (2013).
48. Iwakura, Y., Ishigame, H., Saijo, S. & Nakae, S. Functional Specialization of Interleukin-17 Family Members. *Immunity* vol. 34 149–162 (2011).
49. Gaffen, S. L. Structure and signalling in the IL-17 receptor family. *Nature Reviews Immunology* vol. 9 556–567 (2009).
50. Shi, Y. *et al.* IL-21 Induces an Imbalance of Th17/Treg Cells in Moderate-to-Severe Plaque Psoriasis Patients. *Front Immunol* **10**, 1865 (2019).

51. Jamshidian, A., Shaygannejad, V., Pourazar, A., Zarkesh-Esfahani, S. H. & Gharagozloo, M. Biased Treg/Th17 balance away from regulatory toward inflammatory phenotype in relapsed multiple sclerosis and its correlation with severity of symptoms. *J Neuroimmunol* **262**, 106–112 (2013).
52. Longhi, M. S. *et al.* Inhibition of Interleukin-17 Promotes Differentiation of CD25⁺ Cells Into Stable T Regulatory Cells in Patients With Autoimmune Hepatitis. *Gastroenterology* **142**, (2012).
53. Talaat, R. M., Mohamed, S. F., Bassyouni, I. H. & Raouf, A. A. Th1/Th2/Th17/Treg cytokine imbalance in systemic lupus erythematosus (SLE) patients: Correlation with disease activity. *Cytokine* **72**, (2015).
54. Chaudhry, A. *et al.* CD4⁺ regulatory T cells control TH17 responses in a Stat3-dependent manner. *Science* **326**, 986–91 (2009).
55. Kluger, M. A. *et al.* Treg17 cells are programmed by Stat3 to suppress Th17 responses in systemic lupus. *Kidney Int* **89**, 158–166 (2016).
56. Koenen, H. J. P. M. *et al.* Human CD25^{high}Foxp3^{pos} regulatory T cells differentiate into IL-17 producing cells. *Blood* **112**, 2340–2352 (2008).
57. Remedios, K. A. *et al.* The TNFRSF members CD27 and OX40 coordinately limit TH17 differentiation in regulatory T cells. *Sci Immunol* **3**, eaau2042 (2018).
58. Bovenschen, H. J. *et al.* Foxp3 regulatory T cells of psoriasis patients easily differentiate into IL-17A-producing cells and are found in lesional skin. *Journal of Investigative Dermatology* **131**, 1853–1860 (2011).

59. Remedios, K. A. *et al.* The TNFRSF members CD27 and OX40 coordinately limit TH17 differentiation in regulatory T cells. *Sci Immunol* **3**, eaau2042 (2018).
60. Liu, X. *et al.* Elevated Levels of CD4+CD25+FoxP3+ T Cells in Systemic Sclerosis Patients Contribute to the Secretion of IL-17 and Immunosuppression Dysfunction. *PLoS One* **8**, e64531 (2013).
61. Lee, S. Y. *et al.* IL-1 receptor antagonist (IL-1Ra)-Fc ameliorate autoimmune arthritis by regulation of the Th17 cells/Treg balance and arthrogenic cytokine activation. *Immunol Lett* **172**, 56–66 (2016).
62. Cretney, E., Kallies, A. & Nutt, S. L. Differentiation and function of Foxp3+ effector regulatory T cells. *Trends Immunol* **34**, 74–80 (2013).
63. Romano, M., Fanelli, G., Albany, C. J., Giganti, G. & Lombardi, G. Past, present, and future of regulatory T cell therapy in transplantation and autoimmunity. *Frontiers in Immunology* vol. 10 43 (2019).
64. Tanaka, A. & Sakaguchi, S. Targeting Treg cells in cancer immunotherapy. *Eur J Immunol* **49**, 1140–1146 (2019).

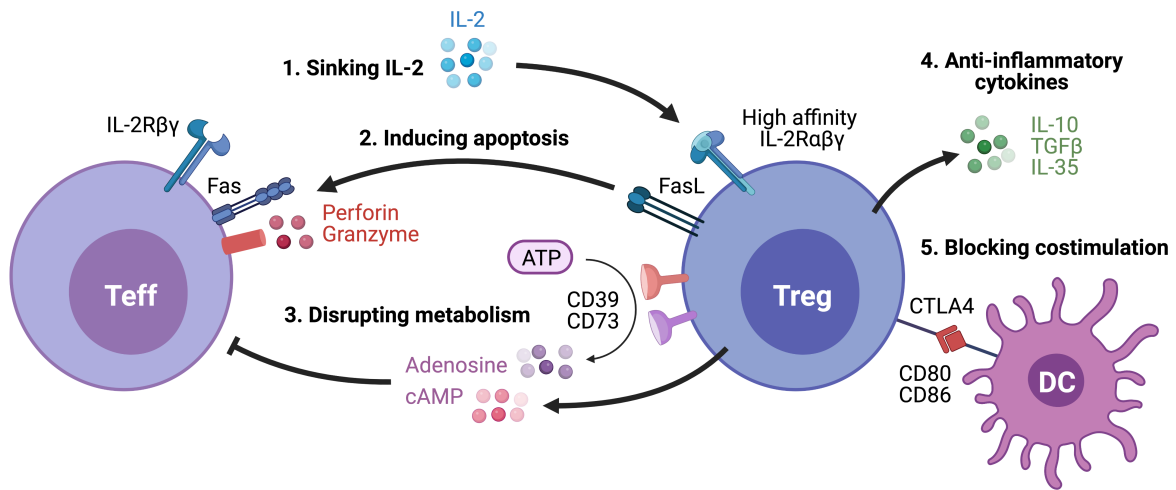


Figure 1.1 Mechanisms of regulatory T cell (Treg) suppression

Tregs can suppress CD4⁺ effector T cell (Teff)-mediated inflammation by multiple direct and indirect mechanisms. Teffs require continuous IL-2 signaling for proliferation and survival **(1)**. Tregs preferentially bind IL-2 using the high-affinity IL-2Rα receptor (CD25) and serve as an IL-2 sink. Tregs can induce Teff apoptosis through FasL-Fas interactions or the release of perforin and granzyme **(2)**. Tregs can disrupt Teff metabolism to inhibit effector function **(3)**. Tregs convert adenosine triphosphate (ATP) to adenosine using ectonucleotidase CD39 and CD73. Tregs can also transfer cyclic adenosine monophosphate (cAMP) directly to Teffs through gap junctions. Tregs release anti-inflammatory cytokines IL-10, IL-35, and TGFβ (transforming growth factor beta) **(4)**. Tregs use CTLA4 to block co-stimulation on antigen presenting cells (APCs) such as dendritic cells (DCs). CTLA4 binds and endocytoses CD80/CD86 on APCs, preventing Teff binding through CD28 **(5)**.

CHAPTER 2: Decoy receptor IL-1R2 in tumor-associated Treg biology

2.1 Introduction

Regulatory T cells (Tregs) are a suppressive immune cell population and key inhibitors of anti-tumor immunity. Low CD8:Treg ratios are associated with poor outcomes in a variety of cancers¹⁻³. Treg depletion can bolster tumor immune rejection, but risks generating systemic autoimmunity⁴⁻⁶. Tregs can inhibit effector T cells through sinking of survival factor IL-2 or release of anti-inflammatory cytokines TGF- β and IL-10⁷. In addition to modifying the local cytokine milieu, we increasingly appreciate that Tregs are activated by inflammatory cytokines, such as TNF α and TLR agonists⁸⁻¹⁰. Manipulating the local cytokine environment could be used to limit inflammation-induced Treg activation in tumors.

IL-1 is a potent inflammatory cytokine with complex biology in tumors. IL-1 β expression can be induced on myeloid populations, while IL-1 α is also produced by healthy mesenchymal cells. Chronic IL-1 signaling can promote keratinocyte hyperproliferation and skin carcinogenesis. In early tumor growth, IL-1 β induces angiogenesis via VEGF and invasiveness through metalloproteinases. At the same time, IL-1 β bolsters adaptive immunity by inducing effector function in CD4⁺ T helper cells (Tconv) and antigen-specific CD8⁺ T cells^{11,12}. A large clinical trial found that anti-IL-1 β treatment (canakinumab) reduced the incidence of tumors over several years¹³. The competing effects of IL-1 β are likely mediated by different cell types¹⁴. While IL-1 signaling on CD4⁺ T conventional cells (Tconv) has been studied extensively¹⁵⁻¹⁹, the role of IL-1 signaling on Treg biology is still an active area of study. IL-1 β in concert with other cytokines can increase effector functions and cytokine production of Tregs *in vitro*, but these results are difficult to replicate *in vivo*^{20,21}.

Due to its broad pro-inflammatory effects, IL-1 signaling is tightly regulated at the systemic and tissue level (**Figure 2.1**). IL-1 α or β bind IL-1 receptor 1 (IL-1R1), which forms a heterodimer with IL-1 receptor associated protein (IL-1RAP or IL-1R3). The heterodimer signals via cytoplasmic Toll/IL-1 receptor (TIR) domains to initiate a signaling cascade including MYD88 (myeloid differentiation primary response gene 88), IRAK1/4 (interleukin-1 receptor activated protein kinase 1 and 4), and TRAF6 (tumor necrosis factor receptor-associated factor 6). This signaling activates transcription factors NF- κ B (Nuclear factor kappa-light-chain-enhancer of activated B cells (NF- κ B) and AP-1 (activator protein 1), among others²². IL-1 receptor antagonist (IL-1RA) competitively inhibits IL-1R1 and prevents the formation of a signaling heterodimer. IL-1 receptor 2 (IL-1R2) lacks an intracellular signaling domain and serves as a sink or decoy receptor for both IL-1 β and IL-1RAP. IL-1R2 can exist in soluble form due to alternative splicing or proteolytic cleavage by metalloproteases²³. While both *Il1ra*^{-/-} and *Il1r2*^{-/-} mice show increased tissue inflammation in arthritis, only IL-1RA deletion increases the risk of systemic shock²⁴⁻²⁶. This distinction suggests that IL-1R2 primarily functions at a local tissue level.

Single cell RNA sequencing (scRNAseq) has identified a subset of IL-1R2 expressing Tregs in mouse and human cancers²⁷⁻³⁰. Characterization of suppressive tumor Tregs has shown IL-1R2 is co-expressed with several markers of suppressive tumor Tregs including 4-1BB, but its function has not been examined^{31,32}. As such, IL-1R2 has been labeled as a marker of tumor Tregs³³. TCR activation can induce IL-1R2 expression on circulating human Tregs *in vitro* but has not been examined in tissue-resident or tumor-infiltrating cells³⁴. Though IL-1R2 expression and structure are highly evolutionarily conserved between mouse and human³⁵, its role in tumor biology is currently unknown.

Here, we characterize a subset of suppressive IL-1R2⁺ Tregs across a variety of human tumors and in a syngeneic mouse model of colon cancer. We identified the factors that promote IL-1R2 expression on tumor-infiltrating Tregs. We show that IL-1R2 attenuates tumor growth by limiting IL-1 signaling on the most activated Tregs. A depleting IL-1R2 antibody was able to selectively reduce tumor-infiltrating Tregs. Leveraging our understanding of IL-1R2 function on Tregs, we have defined a novel therapeutic approach to augment tumor immunity and treat cancer.

2.2 Suppressive Tregs highly express IL-1R2 in human tumors

To identify the genes that define tumor-infiltrating Tregs in human cancer, we sort purified Tregs and Tconv cells from metastatic melanoma tumors and subjected them to bulk RNA sequencing. These samples were matched from our previously published data on CD8⁺ T cells in melanoma³⁶. *IL1R2* was one of the most differentially enriched genes in Tregs vs. Tconv cells by fold change and significance, with high RNA counts in tumor-infiltrating Tregs but almost no expression in tumor-infiltrating Tconv cells from the same patients (**Figure 2.2A, B**). To identify whether *IL1R2* was heterogeneously expressed across tumor Tregs, we re-analyzed our scRNAseq from the same melanoma cohort³⁶. *IL1R2* was expressed across all Tregs (CD4⁺FOXP3⁺), with minimal expression across Tconv (CD4⁺FOXP3⁻) or CD8⁺ T cells (**Figure 2.2C**). These IL1R2⁺ Tregs also showed high expression of *TNFRSF9* (4-1BB), a T cell costimulatory receptor and immune checkpoint associated with Treg suppressiveness in cancer³⁷⁻⁴⁰. To examine IL1R2 expression across tumors more broadly, we integrated scRNAseq data from 46 mixed breast, colorectal, lung, and ovarian cancers in Qian et al. (2020)³². After subsetting on Tregs and re-clustering the dataset, we observed a cluster significantly enriched for

IL1R2 (Cluster 1) (**Figure 2.2D**). Treg cluster 1 was also highly enriched for *TNFRSF9* (4-1BB) and *TNFRSF4* (OX40), a T cell costimulatory receptor (**Supp. Figure 2.9A**)^{37,41-43}. This gene expression profile matched top candidates in the suppressive Treg signature in non-small cell lung cancer described by Guo et al. (2018) and the pan-cancer tumor-reactive Treg signature described by Zheng et al. (2021)^{44,45}. We applied this suppressive signature of *IL1R2*, *TNFRSF9*, and *TNFRSF4* to the Cancer Genome Atlas (TCGA) and performed gene set variation analysis to identify cancers enriched for suppressive tumor Tregs^{46,47}. We observed enrichment of IL1R2⁺ suppressive Tregs in 20 of 33 cancer cell types, including many carcinomas of the gastrointestinal tract (**Figure 2.2E**). Taken together, sequence data from our melanoma patient cohort and the available literature suggest that *IL1R2* is preferentially expressed on a highly activated (and putatively highly suppressive) subset of Tregs across multiple human cancers.

To investigate IL-1R2 expression in mouse Tregs, we bred the Foxp3-IRES-mRFP Treg reporter mouse to the EGFP-knock-in *Il1r2*^{-/-} reporter strain^{48,49}. When heterozygous (EGFP/+), these mice contain one functioning allele of *Il1r2*, and EGFP in place of the other allele (**Supp. Figure 2.9C**). We subcutaneously (s.c.) injected dual-reporter mice with MC38 cells, a syngeneic colon adenocarcinoma line derived from C57Bl/6 mice⁵⁰. MC38 cells produce a “hot tumor” that is rich with immune infiltrate and responds to immunomodulatory treatments⁵¹⁻⁵⁴. We harvested tumors, adjacent skin, and skin draining lymph nodes (sdLN) at multiple timepoints for flow cytometry (**Figure 2.2F, G**). We observed a marked increase in IL-1R2 expression on tumor Tregs over the time course of the experiment (**Figure 2.2H**). We observed minimal to no expression of IL-1R2 on Tconv cells across the time course. In these experiments, approximately 75% of tumor Tregs expressed IL-1R2, with an average 30% expression observed on skin resident Tregs and 15% in tumor-draining lymph node Tregs (tdLN, i.e., inguinal and

axillary lymph nodes on the left side) (**Figure 2.2I**). We stained the same samples with anti-mouse IL-1R2 antibody clone 4E2, the only commercially available monoclonal validated for flow cytometry, and observed significantly lower expression of IL-1R2 in tumor Tregs (~25%). This discrepancy is partially explained by IL-1R2 that is released from cells rather than membrane bound,⁵⁵⁻⁵⁸ and poor antibody affinity. We note the use of either Il1r2-EGFP reporter or anti-IL-1R2 antibody staining in all successive flow cytometry data.

Lastly, we subdivided Tregs by IL-1R2 EGFP reporter expression into low or high expressing cells and compared the expression of Treg effector molecules. In tumors, IL-1R2⁺ Tregs showed significantly higher expression of 4-1BB compared to IL-1R2⁻ Tregs, with no difference in other tissues (**Figure 2.2J**). Similarly, we observed significantly higher PD-1 expression among IL-1R2⁺ Tregs in both the tumor and tdLN (**Figure 2.2K**), which is associated with chronic antigenic stimulation⁵⁹. Taken together, these results suggest that Tregs in mouse tumors preferentially upregulate IL-1R2 progressively with tumor growth, likely in response to significant and prolonged activation.

2.3 IL-1R2⁺ tumor Tregs are not predominantly derived from adjacent skin

We consistently observe a subset of IL-1R2⁺ Tregs in adult mouse skin, with similar levels of receptor expression between tumor-adjacent skin, and contralateral (unaffected) skin (**Supp. Figure 2.10D**). This raised the possibility that IL-1R2-expressing tumor Tregs may arise from pre-activated IL-1R2⁺ Tregs that migrate into tumors from adjacent skin; particularly when injecting syngeneic cancer lines into skin. To test this, we bred mice with an inducible Cre recombinase under the Foxp3 promoter (Foxp3-CreER^{T2}) to mice expressing Rosa26-lox-stop-lox-(LSL)-tdTomato (Ai14) strain, permitting fate mapping of Tregs (**Figure 2.3A**)^{60,61}. When

administered intraperitoneally (i.p.), tamoxifen (tam) is metabolized to the active form Z-4-hydroxytamoxifen (4OHT) by the liver, and induces tdTomato expression in Tregs systemically (**Figure 2.3D Inset**)⁶². By contrast, when we apply topical 4OHT to shaved skin, we can selectively label skin Tregs and track their migration to other tissues. We treated mice with topical 4OHT to the left skin and topical vehicle (acetone) to the right for five consecutive days, then injected MC38 cells bilaterally (**Figure 2.3B**). We harvested tumors, tdLN, and treated skin on Day 21 for flow cytometric analysis. Topical 4OHT labeled approximately 40% of Tregs with tdTomato in the left skin, but only 2% of Tregs in tdLN, ipsilateral tumor, and contralateral tumor (**Figure 2.3C, D**). The majority of Tregs in MC38 tumors are not derived from adjacent skin and may have originated as circulating Tregs, which do not express significant IL-1R2. This finding, along with our kinetic data in Figure 2.1H suggests that Tregs upregulate IL-1R2 once in the tumor microenvironment (TME), likely in response to local inflammation.

2.4 Tumor Tregs upregulate IL-1R2 in response to TCR stimulation but not IL-1 family members

To better understand the factors that promote IL-1R2 expression on Tregs, we first cultured sorted Tregs from the spleen and lymph nodes of Foxp3-RFP, Il1r2-EGFP/+ dual-reporter mice. We observed that TCR stimulation using anti-CD3/CD28 beads caused a progressive increase in Treg IL-1R2 expression over 48 hours in culture (**Figure 2.4A**). This finding is consistent with previous work on human Tregs in culture³⁴. When we further subdivided these Tregs by IL-1R2-EGFP expression and observed that IL-1R2⁺ cells were significantly enriched for 4-1BB (**Figure 2.4B**), consistent with the Treg activation module we observed in human tumors (**Figure 2.2**). In myeloid cells, IL-1R2 expression is increased in

response to local IL-1 β and this acts to attenuate IL-1 signaling through the canonical IL-1 receptor on adjacent cells^{63,64}. Thus, we tested whether Treg expression of IL-1R2 was influenced by local IL-1 β . Lymph node and splenic Tregs were isolated and treated *ex vivo* with increasing concentrations of IL-1 β and IL-1 α for 48 hours. Tregs are typically cultured with high concentrations of anti-CD3/CD28 to increase cell count and viability^{65,66}, but the strong TCR signaling causes most Tregs to express IL-1R2 and could mask any effect of exogenously added IL-1. To overcome this limitation, we cultured Tregs in either a mixed population of lymphocytes without anti-CD3/CD28 beads (**Figure 2.4C**) or cultured Tregs alone with suboptimal TCR stimulation (1:10 bead to cell ratio) (**Figure 2.4D**). Under either condition we did not observe a significant increase in IL-1R2 expression. Similarly, we observed an increase in IL-1R2 expression on human Tregs (hTregs) isolated from peripheral blood following TCR stimulation (**Supp. Figure 2.11B**), but no change in expression with the addition of IL-1 β to cultured hTregs from a lymph node containing a metastatic melanoma lesion (**Supp. Figure 2.11C**). Because Tregs isolated from lymphoid organs may not accurately represent the biology of tissue-resident Tregs *in vivo*, we injected IL-1 β subcutaneously into the back skin of healthy mice and harvested treated skin for flow cytometry analysis. We observed a rapid influx of neutrophils 24 hours after injection, confirming that the IL-1 β had generated local inflammation (**Figure 2.4E, Supp. 2.11D**). Interestingly, this treatment had no effect on IL-1R2 expression on skin Tregs (**Figure 2.4F**). Thus, results from both *ex vivo* and *in vivo* experiments suggest, that unlike in myeloid cells, IL-1 α or IL-1 β are not sufficient to increase IL-1R2 expression on Tregs. These cytokines may still play a role in IL-1R2 upregulation in concert with other factors, but not independently.

To confirm that IL-1R2 expression is induced on Tregs by signaling through the TCR, we bred Foxp3-CreER^{T2} mice with Tera-flox mice. In heterozygous animals (flox/+), tamoxifen

treatment deletes one allele of TCR α in all Tregs. Due to allelic exclusion at the TCR locus, approximately half of Tregs will lose TCR α expression and consequently TCR β , which can be detected by antibody staining⁶⁷⁻⁶⁹. We treated all mice with i.p. tamoxifen, injected MC38 cells and then harvested tumors and tdLN for flow cytometry on Day 21 (**Figure 2.4G**). We subdivided Tregs based on TCR β expression, with each mouse serving as an internal control (**Figure 2.4H**). The TCR β^+ group was most likely larger than 50% due to the generation of new Tregs after tamoxifen treatment. We observed a significant decrease in IL-1R2 antibody staining among TCR β^- Tregs compared to TCR β^+ Tregs in both tdLN (**Figure 2.4I, J**) and tumor (**Figure 2.4K, L**). The lower baseline expression of IL-1R2 on tumor Tregs compared to previous experiments may reflect the earlier timepoint of analysis (14 days post-MC38 implantation). These results demonstrate that TCR signaling *in vivo* plays a major role in inducing IL-1R2 expression on tumor-infiltrating Tregs.

2.5 IL-1R2 expression on Tregs results in reduced tumor growth *in vivo*

The function of IL-1R2 as a decoy receptor on myeloid cells has been previously described^{70,71}. However, it is currently unknown how expression of this receptor influences Treg biology. Because IL-1 β is a potent pro-inflammatory cytokine that can augment anti-tumor immunity⁷², we hypothesized that Treg expression of IL-1R2 acts as a local ‘sink’ for IL-1 β , effectively reducing Tconv cell function. Thus, we reasoned that deletion of IL-1R2 on Tregs would result in increased anti-tumor immunity and reduced tumor growth. Alternatively, IL-1R2 could act in a cell intrinsic manner and affect Treg function directly. To test these hypotheses, we bred Foxp3-CreER^{T2} mice to Ilr2-flox mice to permit inducible deletion of IL-1R2 on Tregs^{26,61}. We treated mixed male and female littermates with tamoxifen or vehicle, then injected MC38

cells in the left flank. We measured tumor volume every other day from Day 8 to 22, and harvested tissues on Day 24 (**Figure 2.5A**). In contrast to our hypothesis, we observed significantly increased tumor growth in mice with IL-1R2 deleted on Tregs compared to controls (**Figure 2.5B**). The effect was observed in both male and female mice, although we observed sex differences in tumor size (**Figure 2.5C**). Flow cytometry at Day 24 confirmed reduction of IL-1R2 antibody staining among Tregs in the tdLN, adjacent skin, and tumor (**Figure 2.5D, E**). These results suggest that IL-1R2 expression may promote survival and/or the stability of Tregs in the tumor environment by limiting IL-1 signaling in a cell intrinsic manner. To investigate the effect of IL-1R2 on tumor-associated Tregs, we examined expression of key Treg effector molecules by flow cytometry. Mice with IL-1R2 deleted on Tregs showed a significant increase in CTLA4 expression on tdLN and tumor Tregs compared to control mice (**Figure 2.5F, G**). In addition, we observed a similar increase in ICOS expression on IL-1R2-deficient Tregs in the tdLN and skin, but not in tumor, where ICOS expression was high at baseline (**Figure 2.5H, I**). We observed no change in the frequency or absolute number of Tconv or CD8⁺ cells (**Supp. Figure 2.12B-E**). To confirm that the increase in tumor growth was not due to tamoxifen or Cre recombinase itself, we repeated the experiment with mice bearing a constitutive Foxp3-Cre crossed to Il1r2-Flox, versus Foxp3-Cre only control mice⁷³. We observed a similar increase in tumor growth among Il1r2^{-/-} mice and verified the decrease in IL-1R2 antibody staining by flow cytometry on Day 24 (**Supp. Figure 2.12F-H**). IL-1R2 expression on neutrophils was unaffected, suggesting Treg-specific cre activity (**Supp. Figure 2.12I**). Taken together, these experiments revealed that IL-1R2 deletion on Tregs increases tumor growth and results in greater Treg activation.

2.6 IL-1R2 attenuates Treg activation in tumors

The experiments outlined above suggest that IL-1 signaling may activate Tregs in tumors independent of antigen and that Treg expression of IL-1R2 attenuates this activation. To investigate the effect of IL-1 signaling on tumor-infiltrating Tregs and how IL-1R2 regulates inflammation-induced activation of Tregs *in vivo*, we compared the gene expression profile of wild-type and IL-1R2-deficient Tregs in the same tumor environment. We isolated lymph node and spleen T cells from wild-type CD45.1 mice (Ctrl) and Foxp3-mRFP; Il1r2-EGFP/EGFP dual-reporter mice, which lack *Il1r2* systemically (Il1r2^{-/-}) (**Figure 2.6A**). T cells were transferred into Rag2^{-/-} hosts at a 50:50 ratio to generate mixed chimeras with ~50% of Tregs able to express IL-1R2 and ~50% of Tregs with IL-1R2 genetically deleted^{74,75}. We injected MC38 cells into each Rag2^{-/-} host on Day 14, and harvested tumors on Day 28. Samples were pooled, sorted on Live CD4⁺ T cells, and submitted for 3' scRNAseq (10X genomics). Pooled tdLN from the same mice were also sequenced (**Supp. Figure 2.13A**). We created a custom mouse reference genome with the sequences of EGFP and IRES-mRFP1 appended for alignment. A module score composed of canonical Treg markers (*Foxp3*, *Ctla4*, *Il2ra*, *Icos*) identified Tregs along the bottom edge of the UMAP projection⁷⁶ (**Figure 2.6B**). Feature plots of *Sell* (CD62L), *Cd44*, and *Foxp3* further delineated populations of Tregs, T effector cells (Teffs), and naïve CD4⁺ T cells (**Figure 2.6C**). *Il1r2* was expressed throughout most of the Treg clusters, but not in Tconv clusters. Notably, Il1r2^{-/-} cells can still show *Il1r2* expression by RNA sequencing as Exon 1 is transcribed without modification in the dual-reporter mouse. We subsetted the dataset on Tregs and re-clustered to produce eleven populations (C0-C11) (**Figure 2.6D**). Overlaying Il1r2-EGFP and Foxp3-mRFP expression over the data identifies an even distribution of Il1r2^{-/-} cells from the dual-reporter mice in all clusters except C3 and C8 (**Figure**

2.6E). mRFP expression was low, but consistent with the sparse Foxp3 expression in the dataset. By contrast, EGFP was a top feature with expression in approximately 20% of Tregs (**Supp. Figure 2.13B**). Due to the significant amount of transcript dropout (zero counts) in scRNAseq, we are undercounting the number of Il1r2^{-/-} cells using EGFP and mRFP expression⁷⁷. Flow cytometry analysis of one of the mixed chimeras showed approximately 66:33 distribution of CD45.1⁺ Ctrl cells vs. CD45.2⁺ dual-reporter cells (Il1r2^{-/-}) (**Supp. Figure 2.13A**). This undercounting of Il1r2^{-/-} cells signifies that any expression differences measured between the two populations are likely greater than reported.

We identified the top differentially expressed (DE) genes in Il1r2^{-/-} Tregs compared to Ctrl Tregs using a Wilcoxon rank sum test⁷⁸ (**Figure 2.6F**). The signature for IL-1R2 deletion included several T cell costimulatory receptors (*Ox40*, *Gitr*, *Lfa2*) and Treg effector molecules (*Ctla4*, *Cd25*, *Vimentin*, *Icos*). *Jund* was also a top DE gene, suggesting increased IL-1 signaling on Il1r2^{-/-} Tregs. *Jund* codes for AP-1, a major transcription factor downstream of IL-1R1 activation⁷⁹⁻⁸¹. To identify biological pathways affected by IL-1R2 deletion, we compared the full DE gene list against the REACTOME database using geneset enrichment analysis (GSEA)⁸²⁻⁸⁴ (**Figure 2.6G**). Top gene sets included metabolic and signaling pathways, suggesting that tumor-infiltrating Tregs lacking IL-1R2 have a more activated phenotype than control IL-1R2 expressing Tregs cells. Enriched pathways include ‘Tnfr2 Non Canonical Nf Kb pathway,’ which further suggests increased IL-1 signaling in IL-1R2 deficient Tregs.

To identify differences between the Treg clusters, we created a module score from 10 top DE genes and applied it to our dataset (**Supp. Figure 2.13C**). The module score was positively correlated with UMAP-2, with low expression in clusters C3 and (blue), and high expression in C0 and C5 (red). Cluster C7 had an intermediate module score, but showed the greatest

difference in expression of DE genes between *Il1r2*^{-/-} and Ctrl Tregs (**Supp. Figure 2.13D**). We hypothesized that C7 has intermediate activation and is most sensitive to changes in IL-1 signaling. We performed Branching pseudotime analysis using Slingshot⁸⁵, with C3 on the control cells as a starting point, believing these to be recent entrants into the tumor (**Supp. Figure 2.13E**). Indeed, C7 was predicted to be an intermediate population on the way toward highly activated clusters C0 and C5. These findings suggest that the partially activated cells in C7 are sensitive to IL-1R2 deletion, while cells in C0 and C5 are maximally activated and unaffected by additional stimulation.

We subset and clustered Tregs from tdLN in a similar manner (**Supp. Figure 2.13F**). Most tdLN cells did not express *Il1r2* (**Supp. Figure 2.13G**), and all but one cluster had a low DE gene module score (**Supp. Figure 2.13H**). The absence of this gradient among tdLN tumors suggests that the *Il1r2*^{-/-} phenotype is driven by local factors in the TME. Taken together, these results demonstrate that IL-1R2 expression on Tregs acts to attenuate IL-1-mediated activation of these cells in the tumor microenvironment.

2.7 Depleting IL-1R2 expressing Tregs reduces tumor growth

While Treg depletion therapies can bolster antitumor immunity, the reduction of systemic Tregs produces significant autoimmunity⁴⁻⁶. Depletion approaches that preferentially target tumor-associated Tregs based on the expression of surface molecules, such as CCR8, are currently under active clinical investigation^{27,28,86}. Given that IL-1R2 expression is preferentially induced in tumors, we hypothesized that it could be an effective target for tumor-associated Treg depletion. To test this hypothesis, we generated and screened antibodies with high affinity for human IL-1R2, but not IL-1R1. One high-affinity clone (59353) also bound to the murine IL-

1R2 homolog. The sequence of this antibody clone was fused to mouse-IgG2a (m2A-WT) Fc region to promote antibody effector functions, including antibody-dependent cellular cytotoxicity (ADCC)⁸⁷. To further increase cell depletion, we also generated a modified IgG2a with three mutations (S239D, A330L, I332E) in the C(H)2 portion of the Fc region (m2a-XTM) that had been previously described to enhance ADCC⁸⁸.

To determine if targeting IL-1R2 can enhance antitumor immunity, we injected female C57/Bl6 mice with MC38 cells s.c. in the left flank (**Figure 2.7A**). Seven days later, we began a series of 5 i.p. injections with anti-IL-1R2 (59353-m2a-XTM) or isotype control (m2a-XTM). Treatment with anti-IL-1R2 (59353-m2a-XTM) mAb produced a significant decrease in MC38 tumor volume across the time course, with the greatest difference at Day 27 (**Figure 2.7B, C**). Anti-IL-1R2 significantly increased mouse survival *i.e.*, the time until mice reached tumor endpoint (2cm³). Over half of anti-IL-1R2 treated mice never reached maximum tumor volume by the end of measurement on Day 50 (**Figure 2.7D**). 20% of anti-IL-1R2 treated mice showed complete tumor rejections, compared to 0 of 10 controls (**Supp. Figure 2.14A**), suggesting that IL-1R2⁺ Treg depletion can not only reduce MC38 growth, but also bolster anti-tumor immunity. We observed similar tumor volume and survival differences using the m2a-WT variant (**Supp. Figure 2.14B-D**), indicating that the unmodified IgG2A Fc region is sufficient to generate cell depletion.

We also performed tumor experiments with CT26, a syngeneic mouse colorectal carcinoma cell line derived from BALB/c mice⁵⁰. The CT26 model also generates “hot tumors” with immune cell infiltrate and has been used to study immunomodulatory cancer therapies^{89,90}. Similarly, we injected CT26 cells s.c. into the left flank and began a series of 5 i.p. injections with anti-IL-1R2 or isotype control on Day 9 (**Figure 2.7E**). Anti-IL-1R2 (59353-m2A-WT)

significantly decreased tumor volumes over the time course, with the greatest difference at Day 26 (**Figure 2.7F, G**). Again, anti-IL-1R2 treatment increased mouse survival time compared to control, with median survival extended by 4 days (**Figure 2.7H**). To confirm Treg depletion, we harvested a subset of mice for immunophenotyping on Day 14. Anti-IL-1R2 treatment significantly reduced (~50%) the percentage of tumor Tregs without affecting the frequency of other T cells in the tumor (**Figure 2.7I, Supp. 2.14F**). Importantly, the percentage of Tregs in tdLN and in circulation were not affected, suggesting that IL-1R2⁺ Treg depletion is limited to the TME and does not generate systemic autoimmunity. We did not observe skin inflammation in the depleted group, despite the presence of IL-1R2⁺ Tregs in healthy skin. Further studies to understand the role of IL-1R2 on skin Tregs and to characterize the effects of depleting skin Tregs are warranted.

IL-1R2⁺ Tregs also in the skin and other tissues will require further Furthermore, anti-IL-1R2 treatment preferentially depleting the most activated Tregs, as marked by a decrease in the percentage CCR8⁺ and 4-1BB⁺ Tregs in the tumor, but not in circulation (**Figure 2.7J, K**). The slight, but not significant increase in CCR8 expression on tdLN Tregs may reflect that CCR8 expression is regulated independently from 4-1BB and IL-1R2 expression. CCR8 may therefore mark a compensatory population of alternatively activated Tregs. Taken together, these results suggest that IL-1R2 antibodies can selectively deplete tumor Tregs resulting in reduced tumor growth.

2.8 Discussion

IL-1R2 was first described on myeloid cells and has been well-characterized in the context of arthritis and local tissue inflammation⁹¹. The decoy receptor is expressed on the cell surface or

released to bind free IL-1 family members and can block IL-1 signaling in a cell-intrinsic (cis) or extrinsic (trans) manner^{92,93}. More recently, scRNA seq has identified a subset of *IL1R2* expressing Tregs in human and mouse tumors^{27,28}. *IL1R2* has appeared as a top differentially expressed gene in several datasets and has consequently been labeled as a marker of tumor Tregs without further investigation into the receptor. Other studies have included *IL1R2* in gene signatures of suppressive tumor Tregs primarily defined by *TNFRSF9* (4-1BB) expression^{32,44}. The correlation between *IL1R2* and *TNFRSF9* expression potentially masks a distinct role of *IL1R2* separate from 4-1BB. While the narrow function of *IL1R2* as a decoy receptor is understood, its role in tumor-associated Tregs was still unclear. Answering this question required manipulation of not only *IL1R2* expression, but also of IL-1 signaling on Tregs. In this study we adapted genetic tools developed to study *IL1R2* on myeloid cells for use in Treg biology.

We identified a population of *IL1R2*⁺ Tregs in the skin of healthy and tumor-bearing mice. *IL1R2* expression in the skin was not affected by tumor volume or time since implantation, suggesting that this population is independent from tumor Tregs. To confirm that tumors are not being seeded by skin Tregs that already express *IL1R2*⁺, we used a skin-restricted fate mapping system developed by our group. Topical 4OHT treatment labeled 40% of skin Tregs, and we observed only 2% of labeled Tregs in each of the ipsilateral tumor, contralateral tumor, and tdLN. With maximal skin labeling, we would extrapolate that 5% of tumor-associated Tregs are labeled, suggesting that the skin is not a major contributor of tumor Tregs. This rare population may represent a subset of recirculating tissue Tregs and warrants further study. If these recirculating Tregs retain their CCR8 expression, they could account for the slight increase in CCR8⁺ lymph node Tregs with our depleting antibody therapy. *IL1R2* has

been described to regulate recirculation of Tregs into the thymus⁹², and these labeled cells may be utilizing similar mechanisms for migration.

A growing body of literature suggests that Tregs are activated by inflammatory mediators in tissues to regulate their effector functions in addition to antigen engagement. Our data suggests that in tumors, TCR stimulation induces an activated Treg signature that includes IL-1R2 expression. IL-1R2 on Tregs functions to attenuate further activation by limiting IL-1 signaling in a cell-intrinsic manner. In this way, Treg expression of IL-1R2 regulates the amount of inflammation-induced activation these cells receive in tumors.

IL-1R2 deficient Tregs in tumors showed higher expression of canonical Treg markers used to suppress immunity, suggesting that IL-1 β directly augments Treg function. This finding is consistent with previous findings that IL-1 promotes effector functions of CD4⁺ and CD8⁺ T cells^{11,12}. On Tregs specifically, IL-1 β in concert with other cytokines can augment Treg suppression of Th17 cells in disease⁹⁴. IL-1 signaling also activate myeloid cells, and IL-1R2 has been shown to limit local tissue inflammation in rheumatoid arthritis models^{26,49}. While myeloid-derived IL-1R2 can regulate cells in trans, the decoy receptor likely functions in a cell intrinsic manner on Tregs, as evidenced by significant expression differences between Il1r2^{-/-} and wild-type Tregs in the same animal. Unlike IL-1R2 expressing myeloid cells, Tregs do not secrete IL-1 β , precluding the possibility of an IL-1 negative feedback loop on Tregs. Instead, Tregs are likely integrating cytokine signaling with TCR engagement to regulate their responses.

These IL-1R2 functions may extend to other diseased tissues. We report a subset of IL-1R2 expressing Tregs in mouse skin, suggesting that these cells are experiencing chronic antigen engagement. IL-1R2 may function to limit Treg activation in inflammatory skin lesions,

particularly in response to IL-1 released by injured and proliferating keratinocytes^{95,96}. Further study into the role of IL-1R2 in skin is warranted.

We initially hypothesized that IL-1R2 on Tregs would promote tumor growth by limiting the amount of free IL-1 β available for T effector cells, thus limiting their activation. Tumor-infiltrating Tregs are generally detrimental for anti-tumor immunity, with high Treg frequency associated with poor prognosis in human cancers¹⁻³. Single-cell expression data from a broad cross-section of tumors revealed that IL-1R2⁺ Tregs co-express TNF receptor super family member 4-1BB, which has been shown to bolster Treg suppression and increase tumor growth^{37,39}. We speculated that IL-1R2 on Tregs may have a similar pro-tumor effect. Instead, we observed that *deletion* of IL-1R2 on Tregs increased tumor growth. In these animals, free IL-1 β was acting directly on Tregs rather than effector cells, again suggesting a cell intrinsic role for IL-1R2 on Tregs.

In our mouse scRNAseq, IL-1R2 deleted Tregs showed increased NF- κ B activation, which is downstream of IL-1 signaling. The enriched NF- κ B pathway is associated with TNF receptor 2 (TNFR2), suggesting that IL-1R signaling either synergizes with TNFR2 signaling, or that the two receptors share a converging signaling cascade. TNFR2 engagement promotes cell survival in highly activated T cells. On Tregs specifically, TNFR2 stabilizes Foxp3 expression and maintains a suppressive phenotype in inflamed tissues⁹⁷. This function carries over to tumors, where TNFR2⁺ Tregs are highly suppressive and promote tumor immune evasion⁹⁸. We speculate that TNFR2-mediated non-canonical NF- κ B activation may be particularly important to retain Treg identity during cytokine exposure in the tumor. While IL-1 β can promote a Th1/17-like Treg phenotype, pro-inflammatory cytokines in excess could destabilize Foxp3 expression and convert the cells to ex-Tregs.

While IL-1R2⁺ Tregs limit tumor growth compared to IL-1R2-deficient cells, the decoy receptor does not mark a ‘beneficial’ population of tumor-infiltrating Tregs. Indeed, IL-1R2 is expressed on the most suppressive tumor Tregs which inhibit tumor immune rejection. Instead, we propose that IL-1R2 limits excessive inflammation-induced activation on Tregs in tumors. The decoy receptor may protect Tregs from activation-induced cell death⁹⁹, and we noted decreased numbers of Il1r2^{-/-} Tregs compared to wild-type cells in our bone marrow chimeras. Any change in Treg survival was not enough to overcome the increased suppressiveness of these cells in response to IL-1 mediated activation. Given these findings, we did not see reason to investigate IL-1R2 blocking as a therapeutic approach for cancer.

Selective expression of IL-1R2 on the most suppressive tumor Tregs makes the decoy receptor an appealing target for cell depletion therapy. Treg depletion is an active area of study, with demonstrated potential to promote tumor immune rejection.^{86,100,101} Systemic depletion of Tregs carries a significant risk of autoimmunity^{5,102}, so identifying surface markers that are selective for tumor Tregs is critical to limit side effects. 4-1BB has been proposed as a depletion target, but the molecule is broadly expressed on activated Tconv cells^{103–105}. Depleting anti-CCR8 therapy is currently in phase 1 clinical trials¹⁰⁶. Chemokine receptor CCR8 is highly expressed on suppressive tumor Tregs but not circulating Tregs, and depletion of CCR8⁺ cells amplifies anti-tumor immunity^{107,108}. However, CCR8 expression is also observed in Th2 cells^{109,110}, NK cells¹¹¹, and tissue resident memory (Trm) cells in human skin¹¹². Approximately 50% of αβ T cells in skin are CCR8⁺, including CD8⁺ and CD4⁺ Tconv cells^{113–115}. The effect of depleting these cells is not yet known. By contrast, IL-1R2 is not expressed by any other population of T cell. In mouse skin, only 30% of Tregs express IL-1R2, and these cells are not depleted by our anti-IL-1R2 antibody (clone 59353). These results suggest that IL-1R2 may be a

cleaner marker for tumor Treg depletion than other proposed targets. Additionally, any off-target depletion of myeloid cells would likely strengthen anti-tumor immunity. Tumor-associated neutrophils and macrophages are generally immunosuppressive and are associated with poor survival in cancer¹¹⁶. We observed a partial, but significant decrease in tumor neutrophil count following anti-IL-1R2 antibody treatment (data not shown).

To our knowledge, this study is the first comprehensive investigation of IL-1R2 function in tumor Treg biology. We defined an inflammation-induced activation signature on Tregs that includes IL-1R2 expression. We showed that IL-1R2 on Tregs limits tumor growth, and defined a cell intrinsic mechanism by which Tregs can use IL-1R2 to attenuate IL-1 mediated activation in cancer. These findings are summarized in our proposed model of IL-1R2 on Tregs (**Figure 2.8**). Cancer cells express self-antigens that can be recognized by Tregs. Continuous antigen engagement via the TCR induces IL-1R2 expression on Tregs. Immunologically “hot” tumors also contain tumor associated macrophages (TAMs), neutrophils, and other myeloid cells that produce IL-1 β . Membrane-bound IL-1R2 binds free IL-1 β and IL-1RAP on the same cell to inhibit IL-1R signaling. Deleting IL-1R2 on Tregs results in increased IL-1R signaling and NF- κ B activity. While soluble IL-1R2 released by Tregs could act in trans, Tregs compose a relatively small fraction of cells in tumors. NF- κ B promotes the expression of multiple Treg effector genes, including *Il2ra* and *Ctla4*, that allow the cells to suppress CD8⁺ and CD4⁺ Teff activity. High affinity IL-2R α reduces the free IL-2 available to Teff cells, while CTLA4 binds CD80/CD86 on antigen-presenting cells (APCs) to prevent Teff binding through CD28. Lastly, we exploited the specificity of IL-1R2 on tumor Tregs to develop a novel cell depleting approach for cancer. Future clinical trials will be needed to determine the safety and efficacy of this approach.

2.9 Methods

Animals

All animals were bred and maintained in a specific pathogen free mouse facility in accordance with the Laboratory Animal Resource Center and Institutional Animal Care and Use Committee of the University of California San Francisco (UCSF). Mice were socially housed under a 12-hour day/night cycle. Littermate controls were used for all experiments except for tumor experiments utilizing Foxp3-Cre; Il1r2-Flox mice vs. Foxp3-Cre Only controls. Animals of both sexes were used, unless otherwise noted. Sex, parental cage, and weaning cage were randomized among experimental groups. All experiments were conducted using adult mice aged 6-18 weeks. Mouse strains used in this study include Foxp3-IRES-mRFP (Jax:008374); Foxp3-GFP-CreERT2 (Jax:016961); Rosa26-LSL-tdTomato [Ai14] (Jax:007914); Foxp3-YFP-Cre (Jax:016959); Cd4-Cre Tg (Jax:022071); Il1r1-Flox (Jax:028398); B6 CD45.1 (Jax:002014); C57Bl/6 (Envigo:057); Balb/C (Envigo:047); (Il1r2-EGFP (kindly provided by Dr. Yoichiro Iwakura); Il1r2-Flox (kindly provided by Dr. Cem Gabay); Tcra-Flox (kindly provided by Dr. Daniel Mucida).

Administration of Tamoxifen, 4OHT, and IL-1 β

Tamoxifen (Sigma-Aldrich) was dissolved in corn oil (Sigma-Aldrich) at 37C by shaking overnight. For systemic Cre recombinase induction, tamoxifen was administered to mice intraperitoneally at a dose of 100 mg/kg every day for 5 days. For tumor growth experiments using Foxp3-CreERT2 mice, we administered additional injections of tamoxifen or vehicle (corn oil) every 6 days to induce Cre recombination in newly generated cells. In experiments using

topical z-4-Hydroxytamoxifen (Sigma-Aldrich), 5 mg of 4OHT was dissolved in 10 ml of acetone (Sigma-Aldrich) to generate a stock concentration of 500 µg/ml. 4OHT was then diluted with acetone to generate working aliquots of 20 µg/ml (1:25 dilution) stored at -80C. We applied 100 µl of 4OHT or vehicle (acetone) to anesthetized mice in a dropwise manner to exposed dorsal back skin over 5 consecutive days. Mice were shaved in a “mohawk” configuration (no depilation was performed), with back skin divided into a left section treated with 4OHT and a right section treated with acetone. Due to the high vapor pressure of acetone, there is no residual liquid to remove from the skin and the mice are returned to their cage.

In experiments with subcutaneous (s.c.) IL-1β injection, we shaved a 3 x 3 cm square on the left back skin of Il1r2-EGFP/+ reporter mice. We resuspended recombinant mouse IL-1β (R&D) at 2 µg/ml and injected 100 µl of IL-1β (200 ng) or PBS control into the center of the shaved region. The shaved region of skin and sdLN were harvested after 24 or 48 hours, as described above.

Adoptive T cell transfer

B6 CD45.1 or Foxp3-RFP; Il1r2-EGFP (CD45.2) mice were euthanized, and inguinal, brachial, axillary, and mesenteric lymph nodes were harvested, pooled by strain, and mashed through a 40 µm strainer using a 5 mL syringe plunger and strained into 5ml of cold RPMI. Cells were spun down and resuspended in 1 ml of 2% FBS/PBS. Spleens were harvested separately as above, but resuspended in 3 ml of PharmLyse 1x (BD) and incubated at 37C for 3 minutes. Lysis was quenched with 12 ml of cold 2% FBS/PBS. Spleen cells were spun down and resuspended in 1 ml of 2% FBS/PBS and combined with lymph node cells. Cells were stained with fluorescent antibodies for TCRβ, CD4, CD8a, CD25, CD62L (1:100) and Ghost viability dye (1:500), then

sorted on a BD FACS Aria 2 as described below. We collected Tregs, CD4⁺ Tconv cells, and CD8⁺ T cells at a ratio of 25:25:50, respectively, and then combined cells from both strains (CD45.1 and Foxp3-RFP;Il1r2-EGFP) at a ratio of 50:50. We resuspended the cell mixture in sterile PBS at 5×10^6 cells/ml, and immediately injected 5×10^5 cells (100 μ l) retro-orbitally into each recipient Rag2^{-/-} host.

Tissue Processing

Mice were euthanized and whole back skin was shaved. For lymph node samples, we dissected either bilateral axillary, brachial, and inguinal lymph nodes (sdLN collectively) or inguinal and axillary nodes ipsilateral to subcutaneous tumors (tdLN collectively). Lymph nodes were mashed through a 40 μ m filter with a 5 mL syringe plunger into cold RPMI. Cells were spun down and resuspended in 500 μ l of 2% FBS/PBS for antibody staining. Tumors were carefully separated from underlying skin, weighed, and finely minced with scissors. Samples were placed in 50 ml conical tubes containing 1-3 mL of C10 digestion media (RPMI with 10% calf serum, 1% HEPES, 1% non-essential amino acids, 1% GlutaMAX, 1% penicillin-streptomycin, 2 mg/mL collagenase XI, 0.5 mg/mL hyaluronidase, and 0.1 mg/mL DNase) and digested in a bacterial shaker for 45 min at 37C and 225 rpm. For back skin, we removed any remaining scapular or inguinal fat before weighing and finely mincing the tissue. Samples were placed in 50 ml conical tubes containing 3 mL of digestion media and digested for 45 min at 37C and 225 rpm. Tumor and skin digestion was quenched with 10 mL of cold RPMI. Samples were vortexed for 10 s and immediately passed through 40 μ m strainers. Cells were spun down and resuspended in 1 mL of 2% FBS/PBS for antibody staining.

Flow Cytometry

Samples were diluted based on cell number, as calculated using a NucleoCounter (ChemoMetec). Single-cell suspensions were pelleted and resuspended in 2% FBS/PBS containing fluorophore-conjugated antibodies listed in the key resources table. Cells were initially stained with antibodies targeting cell surface proteins and Ghost 510 viability dye (Tonbo Biosciences) for 30 min. For intracellular staining, cells were fixed and permeabilized using the Cytofix/Cytoperm kit (BD Biosciences) for 30 min. Samples were resuspended in 2% FBS/PBS for flow analysis on a BD Fortessa. We added CountBright absolute counting beads (Invitrogen) to skin and tumor samples to calculate cells/gram. For cell sorting, we resuspended samples in 25% FBS/DMEM and used a BD FACS Aria2.

For all cell types, initial forward scatter vs. side-scatter gates were carefully adjusted by backgating on live CD45⁺ populations to include immune cells and exclude debris. Strict dead cell and doublet exclusion was performed prior to gating for immune cells (CD45⁺). $\alpha\beta$ T cells were gated as CD45⁺ TCR β ⁺ and subdivided into Tconv (CD4⁺ FoxP3⁻), Treg (CD4⁺ FoxP3⁺), and CD8⁺ T cells (CD8a⁺ CD4⁻). For dual-reporter mice, monomeric red fluorescent protein (mRFP) and enhanced green fluorescent protein (EGFP) were used to report Foxp3 expression and Il1r2 expression, respectively. Neutrophils were gated as CD45⁺ TCR β ⁻ Ly6G⁺ MHC II⁻.

***In vitro* assays**

We isolated cells from the spleen, mesenteric lymph nodes, and skin draining lymph nodes of CD4-Cre; Il1r1-Flox mice or Il1r1-Flox only controls. We enriched for CD4⁺ T cells using an EasySep negative selection kit (StemCell), then sorted Tregs (Live CD25⁺ CD62L⁺) or Tconv cells (Live CD25⁻ CD62L⁻). T cells were expanded in D10F media (DMEM with 10%

calf serum, 1% HEPES, 1% non-essential amino acids, 1% GlutaMAX, 1% sodium pyruvate, 1% penicillin-streptomycin) with fresh 2-mercaptoethanol (55 μ M) and Proleukin (rhIL-2, 2000 IU/ml). For suboptimal TCR stimulation, we added anti-CD3/CD28 Dynabeads (Gibco) at a 1:10 bead:cell ratio, along with varying concentrations of recombinant mouse IL-1 α or IL-1 β (R&D). Cells were collected for flow cytometry or bulk RNA sequencing after 2 days.

For human T cell assays, lymphocytes were extracted from human blood by Ficoll-Paque gradient centrifugation and stained with fluorescent antibodies. We sorted human Tconv cells (Live TCR β^+ CD4 $^+$ CD8a $^-$ CD25 $^-$) and human Tregs (CD25 hi CD127 $^-$). Cells were plated in D10F media with Proleukin 2000 IU/ml and 2:1 anti-CD3/CD28 beads:cells (Gibco). We collected cells after 72 hours for flow cytometry. Melanotic lymph nodes were finely minced with scissors and digested overnight in C10 media with collagenase, hyaluronidase, and DNase. Mixed lymphocytes were counted and plated in D10F media with varying concentrations of recombinant human IL-1 β (R&D) and suboptimal 0.1 μ g/ml anti-CD3/CD28. We collected the lymphocytes after 72 hours, stained for CD4 $^+$ Tconv cells and Tregs, and analyzed by flow cytometry.

MC38 and CT26 tumor growth

IL1R2-specific antibodies were generated via screening of a human IgG yeast display library. Clones were selected with a recombinant fusion of the human IL1R2 full-length extracellular domain (Uniprot P27930 aa 14-343) to the Fc domain of human IgG1. Antibodies were screened for specificity by confirming lack of binding to a human IL1R1 ECD-Fc fusion protein (R&D Systems). We bound high-affinity clone 59353 to mouse-IgG2a (m2A-WT) Fc region to promote antibody-dependent cellular cytotoxicity (ADCC), or to a modified IgG2a

with three mutations (S239D, A330L, I332E) in the C(H)2 portion of the Fc region (m2a-XTM) to further enhance ADCC.

Frozen stocks of MC38 and CT26 tumor cells were provided by Murgencies. Aliquots of cells were thawed and cultured in complete media (DMEM with 10% FBS, 1% sodium pyruvate, 1% GlutaMAX, 1% nonessential amino acids, 1% HEPES, 1% gentamycin sulfate, and 1% penicillin-streptomycin), with passage every other day. For MC38 tumor experiments, we shaved the left flank of C57Bl/6 mice or both flanks for topical 4OHT experiments. Cultured MC38 cells were resuspended in sterile PBS at 5×10^6 cells/ml and placed on ice. We implanted tumors by injecting 100 μ l (5×10^5 cells) or 200 μ l (1×10^6 cells) subcutaneously into the left flank. We measured tumor volume every other day with calipers beginning 8 days after cell injection. Volume was calculated as width (w) * height (h) * (w+h) / 2 and all measurements were taken blind to mouse treatment or genotype. Depleting antibody treatment was initiated on Day 7, when mouse tumors averaged a volume of 100 μ m³. Antibody was injected intraperitoneally every third day until Day 19.

For CT26 tumor experiments, we shaved the left flank of Balb/C mice. Cultured CT26 cells were resuspended in sterile PBS at 2.5×10^6 cells/ml. We injected 200 μ l (5×10^5 cells) subcutaneously into the left flank. We measured tumor volume every other day from Day 8 to Day 26. Depleting antibody treatment was initiated on Day 9, when mouse tumors averaged a volume of 100 μ m³. Antibody was injected intraperitoneally every third day until Day 21.

Single-cell RNA sequencing

We isolated tumor and tdLN from eight Rag2^{-/-} hosts reconstituted with T cells from wild-type mice (B6 CD45.1) and Il1r2^{-/-} mice (Foxp3-RFP, Il1r2-EGFP/EGFP). Samples were

pooled by tissue type and processed as described above. We enriched for CD4⁺ T cells using an EasySep CD4 positive selection kit (StemCell) followed by FACS sorting on Live CD4⁺ cells. We submitted 2 lanes per tissue for single cell RNA sequencing (1x10⁴ cells/lane). Samples were run on separate lanes of a 10X Chromium chip with 3' v2 chemistry (10X Genomics) following manufacturer instructions by the UCSF Institute for Human Genetics Sequencing Core. Libraries were sequenced on an Illumina NovaSeq 6000.

We generated a custom mouse reference genome using the mkref command in Cell Ranger v7.0 (10X Genomics). The custom reference was composed of mm10 (2020A) with the sequences for EGFP and IRES-mRFP1 appended. FastQ files were aligned and filtered using the count command in Cell Ranger v7.0. Downstream data analysis, including clustering, visualizations, and exploratory analyses, were performed in R v4.0 using Seurat package v4.3.0. Cells with <200 features, >2500 reads, > 5% mitochondrial reads, >42% ribosomal reads were filtered out during preprocessing. Datasets were log normalized and integrated using the canonical correlate analysis (CCA) based IntegrateData function, with the top 200 most variable features selected as integration anchors. We ran PCA on the integrated objects and ran the JackStraw function to determine significant principal components (PCs). Based on the JackStraw results, we proceeded with the first 30 PCs for tumor samples A and B, the first 20 PCs for tdLN samples C and D, and the first 40 PCs for combined tumor and tdLN samples A-D. We generated multiple UMAPs per integrated object to determine an optimal clustering resolution. We proceeded with a resolution of 1.0 for tumor, 1.0 for tdLN, and 1.2 for combined tumor and tdLN. Tregs were identified by expression of a Treg module score, composed of *Foxp3*, *Il2ra*, *Ctla4*, *Lrrc32*, *Lag3*, *Pcd1*, *Il10*, *Il1r2*, *Tnfrsf9*, and *Tnfrsf4*. We subset on Tregs, reclustered, and removed any outliers. Cells were categorized as Il1r2^{-/-} if they expressed EGFP and/or

IRES-mRFP or Ctrl if they did not. In the tumor Treg object, clusters C3 and C8 had a low frequency of *Il1r2*^{-/-} cells and were excluded from differential expression (DE) gene analysis. We calculate DE genes between *Il1r2*^{-/-} and Ctrl tumor Tregs using the fast Wilcoxon area under curve function in the Presto package. We performed gene set enrichment analysis (GSEA) using the Fgsea package, with DE genes (sorted by log₂ fold change) as input and Reactome pathways as the comparator. We created an *Il1r2*^{-/-} module out of Top DE genes *Tnfrsf4*, *Tnfrsf9*, *Tnfrsf18*, *Ikzf2*, *Icos*, *Il2ra*, *Vim*, *Cd2*, and *Jund*. We performed trajectory analysis using the Slingshot package, with cluster C3 in the control sample set as the starting point.

Reanalysis of Sequencing Data

For bulk sequencing of human melanoma T cells, we obtained un-normalized gene counts from melanoma Treg and Teff samples in Mahuron et al. (2020). We calculated genes enriched in Tregs vs. Teffs using the DEseq2 package and plotted genes on a volcano plot using the Enhanced Volcano package. For single cell sequencing of melanoma Tregs, we obtained filtered feature matrices of gene expression from patient K409 in Mahuron et al. (2020). We filtered, normalized, and clustered cell using Seurat as described above. We generated feature plots with canonical T cell genes (*CD8A*, *CD4*, *FOXP3*, *TNFRSF9*) to classify cell types, and plotted *IL1R2* expression across the dataset. To compare *IL1R2* expression across human tumors, we used BBrowser (BioTuring) to integrate scRNA seq count data from 46 tumors in Qian et al. (2020) using Harmony with batch correction per patient. We subset the dataset on Tregs and performed Louvain clustering. We overlaid *IL1R2*, *TNFRSF9*, and *TNFRSF4* expression on a t-SNE plot (t-distributed stochastic neighbor embedding) of the dataset to identify a cluster of suppressive Tregs (C1). We compared expression of C1 Tregs to other Tregs and to other Tconv

cells from Qian et al to identify C1-defining genes. To identify the tumors most enriched for these suppressive Tregs, we performed gene set variation analysis (GSVA) using *IL1R2*, *TNFRSF9*, and *TNFRSF4* against 33 cancers from the Cancer Genome Atlas (TCGA).

Quantification and Statistical Analysis

Statistical analyses were performed using Prism v9.4.1 (GraphPad). P-values were calculated using two-tailed unpaired or paired Student's t-tests or one-way ANOVA and as indicated in the figure legends. Mice cohort size was designed to be sufficient to enable accurate determination of statistical significance and no animals were excluded from the statistical analysis. Mice were assigned to treatment or control groups randomly. Apart from bulk and single cell RNAseq, all experiments were repeated 2-3 times, and all data points represent individual biological replicates unless noted otherwise. Experimental schematics were created with BioRender.com.

2.10 References

1. Sato, E. *et al.* Intraepithelial CD8⁺ tumor-infiltrating lymphocytes and a high CD8⁺/regulatory T cell ratio are associated with favorable prognosis in ovarian cancer. *Proc Natl Acad Sci U S A* **102**, 18538–18543 (2005).
2. Baras, A. S. *et al.* The ratio of CD8 to Treg tumor-infiltrating lymphocytes is associated with response to cisplatin-based neoadjuvant chemotherapy in patients with muscle invasive urothelial carcinoma of the bladder. *Oncoimmunology* **5**, (2016).
3. Shah, W. *et al.* A reversed CD4/CD8 ratio of tumor-infiltrating lymphocytes and a high percentage of CD4⁺FOXP3⁺ regulatory T cells are significantly associated with clinical outcome in squamous cell carcinoma of the cervix. *Cellular & Molecular Immunology* *2010 8:1* **8**, 59–66 (2010).
4. Shimizu, J., Yamazaki, S. & Sakaguchi, S. Induction of Tumor Immunity by Removing CD25⁺CD4⁺ T Cells: A Common Basis Between Tumor Immunity and Autoimmunity. *The Journal of Immunology* **163**, 5211–5218 (1999).
5. Kim, J. *et al.* Cutting Edge: Depletion of Foxp3⁺ Cells Leads to Induction of Autoimmunity by Specific Ablation of Regulatory T Cells in Genetically Targeted Mice. *The Journal of Immunology* **183**, 7631–7634 (2009).
6. Jacob, J. B., Kong, Y. M., Nalbantoglu, I., Snower, D. P. & Wei, W.-Z. Tumor Regression following DNA Vaccination and Regulatory T Cell Depletion in neu Transgenic Mice Leads to an Increased Risk for Autoimmunity. *The Journal of Immunology* **182**, 5873–5881 (2009).
7. Shevryev, D. & Tereshchenko, V. Treg Heterogeneity, Function, and Homeostasis. *Front Immunol* **10**, 3100 (2020).

8. Gouirand, V., Habrylo, I. & Rosenblum, M. D. Regulatory T Cells and Inflammatory Mediators in Autoimmune Disease. *Journal of Investigative Dermatology* **142**, 774–780 (2022).
9. Duhon, T., Duhon, R., Lanzavecchia, A., Sallusto, F. & Campbell, D. J. Functionally distinct subsets of human FOXP3⁺ Treg cells that phenotypically mirror effector Th cells. *Blood* **119**, 4430–4440 (2012).
10. Conroy, H., Marshall, N. A. & Mills, K. H. G. TLR ligand suppression or enhancement of Treg cells? A double-edged sword in immunity to tumours. *Oncogene* *2008* **27**:2 **27**, 168–180 (2008).
11. Ben-Sasson, S. Z. *et al.* IL-1 acts directly on CD4 T cells to enhance their antigen-driven expansion and differentiation. *Proc Natl Acad Sci U S A* **106**, 7119–7124 (2009).
12. Ben-Sasson, S. Z. *et al.* IL-1 enhances expansion, effector function, tissue localization, and memory response of antigen-specific CD8 T cells. *Journal of Experimental Medicine* **210**, 491–502 (2013).
13. Ridker, P. M. *et al.* Effect of interleukin-1 β inhibition with canakinumab on incident lung cancer in patients with atherosclerosis: exploratory results from a randomised, double-blind, placebo-controlled trial. *Lancet* **390**, 1833–1842 (2017).
14. Dmitrieva-Posocco, O. *et al.* Cell-Type-Specific Responses to Interleukin-1 Control Microbial Invasion and Tumor-Elicited Inflammation in Colorectal Cancer. *Immunity* **50**, 166-180.e7 (2019).
15. Sutton, C., Brereton, C., Keogh, B., Mills, K. H. G. & Lavelle, E. C. A crucial role for interleukin (IL)-1 in the induction of IL-17-producing T cells that mediate autoimmune encephalomyelitis. *Journal of Experimental Medicine* **203**, 1685–1691 (2006).

16. Santarlaschi, V. *et al.* IL-1 and T helper immune responses. *Front Immunol* **4**, 182 (2013).
17. Chung, Y. *et al.* Critical Regulation of Early Th17 Cell Differentiation by Interleukin-1 Signaling. *Immunity* **30**, 576–587 (2009).
18. Weiss, D. I. *et al.* IL-1 β Induces the Rapid Secretion of the Antimicrobial Protein IL-26 from Th17 Cells. *J Immunol* [ji1900318](https://doi.org/10.4049/jimmunol.1900318) (2019) doi:10.4049/jimmunol.1900318.
19. Shaw, M. H., Kamada, N., Kim, Y. G. & Núñez, G. Microbiota-induced IL-1 β , but not IL-6, is critical for the development of steady-state TH17 cells in the intestine. *Journal of Experimental Medicine* **209**, 251–258 (2012).
20. Basu, R. *et al.* IL-1 signaling modulates activation of STAT transcription factors to antagonize retinoic acid signaling and control the TH17 cell–iTreg cell balance. *Nature Immunology* *2015 16:3* **16**, 286–295 (2015).
21. Li, L., Kim, J. & Boussiotis, V. A. IL-1 β -mediated signals preferentially drive conversion of regulatory T cells but not conventional T cells into IL-17-producing cells. *J Immunol* **185**, 4148–53 (2010).
22. Verstrepen, L. *et al.* TLR-4, IL-1R and TNF-R signaling to NF- κ B: Variations on a common theme. *Cellular and Molecular Life Sciences* **65**, 2964–2978 (2008).
23. Peters, V. A., Joesting, J. J. & Freund, G. G. IL-1 receptor 2 (IL-1R2) and its role in immune regulation. *Brain, Behavior, and Immunity* vol. 32 1–8 (2013).
24. Horai, R. *et al.* Development of chronic inflammatory arthropathy resembling rheumatoid arthritis in interleukin 1 receptor antagonist-deficient mice. *J Exp Med* **191**, 313–20 (2000).

25. Lamacchia, C. *et al.* Distinct Roles of Hepatocyte- and Myeloid Cell-Derived IL-1 Receptor Antagonist during Endotoxemia and Sterile Inflammation in Mice. *The Journal of Immunology* **185**, 2516–2524 (2010).
26. Martin, P. *et al.* Deficiency in IL-1 Receptor Type 2 Aggravates K/BxN Serum Transfer-Induced Arthritis in Mice but Has No Impact on Systemic Inflammatory Responses. *J Immunol* **198**, 2916–2926 (2017).
27. De Simone, M. *et al.* Transcriptional Landscape of Human Tissue Lymphocytes Unveils Uniqueness of Tumor-Infiltrating T Regulatory Cells. *Immunity* **45**, 1135–1147 (2016).
28. Plitas, G. *et al.* Regulatory T Cells Exhibit Distinct Features in Human Breast Cancer. *Immunity* **45**, 1122–1134 (2016).
29. Grinberg-Bleyer, Y. *et al.* NF- κ B c-Rel Is Crucial for the Regulatory T Cell Immune Checkpoint in Cancer. *Cell* **170**, 1096–1108.e13 (2017).
30. Zheng, Y. *et al.* Immune suppressive landscape in the human esophageal squamous cell carcinoma microenvironment. *Nat Commun* **11**, 1–17 (2020).
31. Guo, X. *et al.* Global characterization of T cells in non-small-cell lung cancer by single-cell sequencing. *Nat Med* **24**, 978–985 (2018).
32. Qian, J. *et al.* A pan-cancer blueprint of the heterogeneous tumor microenvironment revealed by single-cell profiling. *Cell Research* **2020 30:9 30**, 745–762 (2020).
33. Molgora, M., Supino, D., Mantovani, A. & Garlanda, C. Tuning inflammation and immunity by the negative regulators IL-1R2 and IL-1R8. *Immunol Rev* **281**, 233–247 (2018).
34. Mercer, F., Kozhaya, L. & Unutmaz, D. Expression and Function of TNF and IL-1 Receptors on Human Regulatory T Cells. *PLoS One* **5**, e8639 (2010).

35. Copeland, N. G. *et al.* Chromosomal location of murine and human IL-1 receptor genes. *Genomics* **9**, 44–50 (1991).
36. Mahuron, K. M. *et al.* Layilin augments integrin activation to promote antitumor immunity. *Journal of Experimental Medicine* **217**, (2020).
37. Hamano, R., Huang, J., Yoshimura, T., Oppenheim, J. J. & Chen, X. TNF optimally activates regulatory T cells by inducing TNF receptor superfamily members TNFR2, 4-1BB and OX40. *Eur J Immunol* **41**, 2010–2020 (2011).
38. Freeman, Z. T. *et al.* A conserved intratumoral regulatory T cell signature identifies 4-1BB as a pan-cancer target. *J Clin Invest* **130**, 1405–1416 (2020).
39. Zheng, G., Wang, B. & Chen, A. The 4-1BB Costimulation Augments the Proliferation of CD4⁺CD25⁺ Regulatory T Cells. *The Journal of Immunology* **173**, 2428–2434 (2004).
40. Long, A. H. *et al.* 4-1BB costimulation ameliorates T cell exhaustion induced by tonic signaling of chimeric antigen receptors. *Nature Medicine* **21**, 581–590 (2015).
41. Gramaglia, I., Weinberg, A. D., Lemon, M. & Croft, M. Ox-40 Ligand: A Potent Costimulatory Molecule for Sustaining Primary CD4 T Cell Responses. *The Journal of Immunology* **161**, 6510–6517 (1998).
42. Zhang, X. *et al.* OX40 Costimulation Inhibits Foxp3 Expression and Treg Induction via BATF3-Dependent and Independent Mechanisms. *Cell Rep* **24**, 607–618 (2018).
43. Bulliard, Y. *et al.* OX40 engagement depletes intratumoral Tregs via activating FcγRs, leading to antitumor efficacy. *Immunol Cell Biol* **92**, 475–480 (2014).
44. Guo, X. *et al.* Global characterization of T cells in non-small-cell lung cancer by single-cell sequencing. *Nature Medicine* **24**, 978–985 (2018).

45. Zheng, L. *et al.* Pan-cancer single-cell landscape of tumor-infiltrating T cells. *Science* **374**, (2021).
46. Wang, Z., Jensen, M. A. & Zenklusen, J. C. A practical guide to The Cancer Genome Atlas (TCGA). *Methods in Molecular Biology* **1418**, 111–141 (2016).
47. Hänzelmann, S., Castelo, R. & Guinney, J. GSVA: Gene set variation analysis for microarray and RNA-Seq data. *BMC Bioinformatics* **14**, 1–15 (2013).
48. Wan, Y. Y. & Flavell, R. A. Identifying Foxp3-expressing suppressor T cells with a bicistronic reporter. *Proc Natl Acad Sci U S A* **102**, 5126–5131 (2005).
49. Shimizu, K. *et al.* IL-1 receptor type 2 suppresses collagen-induced arthritis by inhibiting IL-1 signal on macrophages. *J Immunol* **194**, 3156–68 (2015).
50. Corbett, T. H., Griswold Jr., D. P., Roberts, B. J., Peckham, J. C. & Schabel Jr., F. M. Tumor Induction Relationships in Development of Transplantable Cancers of the Colon in Mice for Chemotherapy Assays, with a Note on Carcinogen Structure. *Cancer Res* **35**, 2434–2439 (1975).
51. Arensman, M. D. *et al.* Anti-tumor immunity influences cancer cell reliance upon ATG7. *Oncoimmunology* **9**, (2020).
52. Efremova, M. *et al.* Targeting immune checkpoints potentiates immunoediting and changes the dynamics of tumor evolution. *Nat Commun* **9**, (2018).
53. Zippelius, A., Schreiner, J., Herzig, P. & Muller, P. Induced PD-L1 expression mediates acquired resistance to agonistic anti-CD40 treatment. *Cancer Immunol Res* **3**, 236–244 (2015).

54. Fabian, K. P., Padgett, M. R., Fujii, R., Schlom, J. & Hodge, J. W. Differential combination immunotherapy requirements for inflamed (warm) tumors versus T cell excluded (cool) tumors: engage, expand, enable, and evolve. *J Immunother Cancer* **9**, e001691 (2021).
55. Orlando, S. *et al.* TNF-alpha, unlike other pro- and anti-inflammatory cytokines, induces rapid release of the IL-1 type II decoy receptor in human myelomonocytic cells. *The Journal of Immunology* **158**, 3861–3868 (1997).
56. Liu, C. *et al.* Cloning and Characterization of an Alternatively Processed Human Type II Interleukin-1 Receptor mRNA. *Journal of Biological Chemistry* **271**, 20965–20972 (1996).
57. Symons, J. A., Young, P. R. & Duff, G. W. Soluble type II interleukin 1 (IL-1) receptor binds and blocks processing of IL-1 beta precursor and loses affinity for IL-1 receptor antagonist. *Proceedings of the National Academy of Sciences* **92**, 1714–1718 (1995).
58. Uchikawa, S. *et al.* ADAM17 regulates IL-1 signaling by selectively releasing IL-1 receptor type 2 from the cell surface. *Cytokine* **71**, 238–245 (2015).
59. Aksoylar, H. I. & Boussiotis, V. A. PD-1+ Treg cells: a foe in cancer immunotherapy? *Nature Immunology* 2020 21:11 **21**, 1311–1312 (2020).
60. Madisen, L. *et al.* A robust and high-throughput Cre reporting and characterization system for the whole mouse brain. *Nature Neuroscience* 2009 13:1 **13**, 133–140 (2009).
61. Rubtsov, Y. P. *et al.* Stability of the regulatory T cell lineage in vivo. *Science (1979)* **329**, 1667–1671 (2010).
62. Lim, C. K. *et al.* A comparative study of tamoxifen metabolism in female rat, mouse and human liver microsomes. *Carcinogenesis* **15**, 589–593 (1994).

63. Madej, M. P., Töpfer, E., Boraschi, D. & Italiani, P. Different regulation of interleukin-1 production and activity in monocytes and macrophages: Innate memory as an endogenous mechanism of IL-1 inhibition. *Front Pharmacol* **8**, 335 (2017).
64. Ma, J. *et al.* Regulation of macrophage activation. *Cellular and Molecular Life Sciences* **60**, 2334–2346 (2003).
65. Collison, L. W. & Vignali, D. A. A. In Vitro Treg Suppression Assays. *Methods in Molecular Biology* **707**, 21–37 (2011).
66. Earle, K. E. *et al.* In vitro expanded human CD4⁺CD25⁺ regulatory T cells suppress effector T cell proliferation. *Clinical Immunology* **115**, 3–9 (2005).
67. Polic, B., Kunkel, D., Scheffold, A. & Rajewsky, K. How $\alpha\beta$ T cells deal with induced TCR α ablation. *Proc Natl Acad Sci U S A* **98**, 8744–8749 (2001).
68. Borgulya, P., Kishi, H., Uematsu, Y. & von Boehmer, H. Exclusion and inclusion of α and β T cell receptor alleles. *Cell* **69**, 529–537 (1992).
69. Krangel, M. S., Weaver, C. & Rudensky, A. Mechanics of T cell receptor gene rearrangement. *Curr Opin Immunol* **21**, 133–139 (2009).
70. Colotta, F. *et al.* Interleukin-1 type II receptor: A decoy target for IL-1 that is regulated by IL-4. *Science (1979)* **261**, 472–475 (1993).
71. Re, F. *et al.* Inhibition of interleukin-1 responsiveness by type II receptor gene transfer: A surface ‘Receptor’ with anti-interleukin-1 function. *Journal of Experimental Medicine* **183**, 1841–1850 (1996).
72. Sun, R., Gao, D. S., Shoush, J. & Lu, B. The IL-1 family in tumorigenesis and antitumor immunity. *Semin Cancer Biol* **86**, 280–295 (2022).

73. Rubtsov, Y. P. *et al.* Regulatory T Cell-Derived Interleukin-10 Limits Inflammation at Environmental Interfaces. *Immunity* **28**, 546–558 (2008).
74. Ferreira, F. M. *et al.* Bone marrow chimeras—a vital tool in basic and translational research. *J Mol Med* **97**, 889–896 (2019).
75. Hao, Z. & Rajewsky, K. Homeostasis of Peripheral B Cells in the Absence of B Cell Influx from the Bone Marrow. *Journal of Experimental Medicine* **194**, 1151–1164 (2001).
76. Stuart, T. *et al.* Comprehensive Integration of Single-Cell Data. *Cell* **177**, 1888–1902.e21 (2019).
77. Kharchenko, P. V., Silberstein, L. & Scadden, D. T. Bayesian approach to single-cell differential expression analysis. *Nature Methods* *2014 11:7* **11**, 740–742 (2014).
78. Korsunsky, I., Nathan, A., Millard, N. & Raychaudhuri, S. Presto scales Wilcoxon and auROC analyses to millions of observations. *bioRxiv* 653253 (2019) doi:10.1101/653253.
79. Vesely, P. W., Staber, P. B., Hoefler, G. & Kenner, L. Translational regulation mechanisms of AP-1 proteins. *Mutation Research/Reviews in Mutation Research* **682**, 7–12 (2009).
80. Josue Ruiz, E. *et al.* JunD, not c-Jun, is the AP-1 transcription factor required for Ras-induced lung cancer. *JCI Insight* **6**, (2021).
81. Ruppert, S. M. *et al.* JunD/AP-1-Mediated Gene Expression Promotes Lymphocyte Growth Dependent on Interleukin-7 Signal Transduction. *PLoS One* **7**, e32262 (2012).
82. Subramanian, A. *et al.* Gene set enrichment analysis: A knowledge-based approach for interpreting genome-wide expression profiles. *Proc Natl Acad Sci U S A* **102**, 15545–15550 (2005).
83. Korotkevich, G. *et al.* Fast gene set enrichment analysis. *bioRxiv* 060012 (2021) doi:10.1101/060012.

84. Fabregat, A. *et al.* The Reactome Pathway Knowledgebase. *Nucleic Acids Res* **46**, D649–D655 (2018).
85. Street, K. *et al.* Slingshot: Cell lineage and pseudotime inference for single-cell transcriptomics. *BMC Genomics* **19**, 1–16 (2018).
86. Tanaka, A. & Sakaguchi, S. Targeting Treg cells in cancer immunotherapy. *Eur J Immunol* **49**, 1140–1146 (2019).
87. Lazar, G. A. *et al.* Engineered antibody Fc variants with enhanced effector function. *Proc Natl Acad Sci U S A* **103**, 4005–4010 (2006).
88. Oganessian, V., Damschroder, M. M., Leach, W., Wu, H. & Dall’Acqua, W. F. Structural characterization of a mutated, ADCC-enhanced human Fc fragment. *Mol Immunol* **45**, 1872–1882 (2008).
89. Stringhini, M., Probst, P. & Neri, D. Immunotherapy of CT26 murine tumors is characterized by an oligoclonal response of tissue-resident memory T cells against the AH1 rejection antigen. *Eur J Immunol* **50**, 1591–1597 (2020).
90. Hutmacher, C., Nuñez, N. G., Liuzzi, A. R., Becher, B. & Neri, D. Targeted delivery of IL2 to the tumor stroma potentiates the action of immune checkpoint inhibitors by preferential activation of NK and CD8 β T cells. *Cancer Immunol Res* **7**, 572–583 (2019).
91. Bonecchi, R., Garlanda, C., Mantovani, A. & Riva, F. Cytokine decoy and scavenger receptors as key regulators of immunity and inflammation. *Cytokine* **87**, 37–45 (2016).
92. Nikolouli, E. *et al.* Recirculating IL-1R2⁺ Tregs fine-tune intrathymic Treg development under inflammatory conditions. *Cell Mol Immunol* **18**, 182–193 (2021).
93. Garlanda, C., Dinarello, C. A. & Mantovani, A. The Interleukin-1 Family: Back to the Future. *Immunity* **39**, 1003–1018 (2013).

94. Kluger, M. A. *et al.* Treg17 cells are programmed by Stat3 to suppress Th17 responses in systemic lupus. *Kidney Int* **89**, 158–166 (2016).
95. Furue, M. & Kadono, T. “Inflammatory skin march” in atopic dermatitis and psoriasis. *Inflammation Research* 2017 *66:10* **66**, 833–842 (2017).
96. Groves, R. W., Mizutani, H., Kieffer, J. D. & Kupper, T. S. Inflammatory skin disease in transgenic mice that express high levels of interleukin 1 alpha in basal epidermis. *Proceedings of the National Academy of Sciences* **92**, 11874–11878 (1995).
97. Chen, X. *et al.* TNFR2 Is Critical for the Stabilization of the CD4+Foxp3+ Regulatory T Cell Phenotype in the Inflammatory Environment. *The Journal of Immunology* **190**, 1076–1084 (2013).
98. Yolcu, E. S. *et al.* Apoptosis as a mechanism of T-regulatory cell homeostasis and suppression. *Immunol Cell Biol* **86**, 650–658 (2008).
99. Van Damme, H. *et al.* Therapeutic depletion of CCR8+ tumor-infiltrating regulatory T cells elicits antitumor immunity and synergizes with anti-PD-1 therapy. *J Immunother Cancer* **9**, e001749 (2021).
100. Onda, M., Kobayashi, K. & Pastan, I. Depletion of regulatory T cells in tumors with an anti-CD25 immunotoxin induces CD8 T cell-mediated systemic antitumor immunity. *Proc Natl Acad Sci U S A* **116**, 4575–4582 (2019).
101. Lees, J. G., Duffy, S. S., Perera, C. J. & Moalem-Taylor, G. Depletion of Foxp3+ regulatory T cells increases severity of mechanical allodynia and significantly alters systemic cytokine levels following peripheral nerve injury. *Cytokine* **71**, 207–214 (2015).
102. Qi, X. *et al.* Optimization of 4-1BB antibody for cancer immunotherapy by balancing agonistic strength with FcγR affinity. *Nature Communications* 2019 *10:1* **10**, 1–11 (2019).

103. Freeman, Z. T. *et al.* A conserved intratumoral regulatory T cell signature identifies 4-1BB as a pan-cancer target. *J Clin Invest* **130**, 1405–1416 (2020).
104. Vinay, D. S. & Kwon, B. S. Immunotherapy of cancer with 4-1BB. *Mol Cancer Ther* **11**, 1062–1070 (2012).
105. A First-in-human Study to Learn How Safe the Study Drug BAY3375968, an Anti-CCR8 Antibody, is, When Given Alone or in Combination With Pembrolizumab, How it Affects the Body, How it Moves Into, Through, and Out of the Body, and to Find the Best Dose in Participants With Advanced Solid Tumors .
<https://clinicaltrials.gov/ct2/show/NCT05537740>.
106. Kidani, Y. *et al.* CCR8-targeted specific depletion of clonally expanded Treg cells in tumor tissues evokes potent tumor immunity with long-lasting memory. *Proc Natl Acad Sci U S A* **119**, e2114282119 (2022).
107. Whiteside, S. K. *et al.* CCR8 marks highly suppressive Treg cells within tumours but is dispensable for their accumulation and suppressive function. *Immunology* **163**, 512–520 (2021).
108. Zingoni, A. *et al.* Cutting Edge: The Chemokine Receptor CCR8 Is Preferentially Expressed in Th2 But Not Th1 Cells. *The Journal of Immunology* **161**, 547–551 (1998).
109. Soler, D. *et al.* CCR8 Expression Identifies CD4 Memory T Cells Enriched for FOXP3+ Regulatory and Th2 Effector Lymphocytes. *The Journal of Immunology* **177**, 6940–6951 (2006).
110. Inngjerdigen, M., Damaj, B. & Maghazachi, A. A. Human NK Cells Express CC Chemokine Receptors 4 and 8 and Respond to Thymus and Activation-Regulated

- Chemokine, Macrophage-Derived Chemokine, and I-309. *The Journal of Immunology* **164**, 4048–4054 (2000).
111. McCully, M. L. *et al.* CCR8 Expression Defines Tissue-Resident Memory T Cells in Human Skin. *The Journal of Immunology* **200**, 1639–1650 (2018).
112. Ebert, L. M., Meuter, S. & Moser, B. Homing and Function of Human Skin $\gamma\delta$ T Cells and NK Cells: Relevance for Tumor Surveillance. *The Journal of Immunology* **176**, 4331–4336 (2006).
113. McCully, M. L. *et al.* Epidermis instructs skin homing receptor expression in human T cells. *Blood* **120**, 4591–4598 (2012).
114. Schaerli, P. *et al.* A Skin-selective Homing Mechanism for Human Immune Surveillance T Cells. *Journal of Experimental Medicine* **199**, 1265–1275 (2004).
115. Hedrick, C. C. & Malanchi, I. Neutrophils in cancer: heterogeneous and multifaceted. *Nature Reviews Immunology* 2021 22:3 **22**, 173–187 (2021).

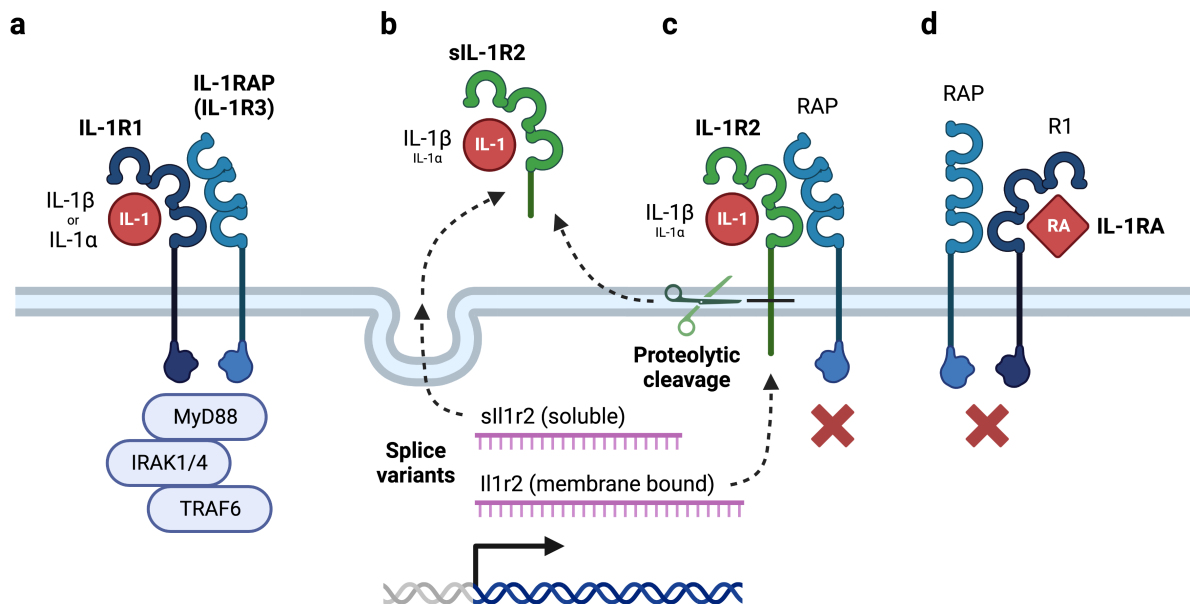


Figure 2.1 Regulation of interleukin-1 (IL-1) signaling

A. IL-1 β or IL-1 α binds IL-1 receptor (IL-1R1), allowing the formation of a heterodimer with IL-1 receptor accessory protein (IL-1RAP or IL-1R3). The heterodimer signals through cytoplasmic Toll/IL-1 receptor (TIR) domains to recruit adaptor proteins MYD88 (myeloid differentiation primary response gene 88), and IRAK1/4 (interleukin-1 receptor activated protein kinase 1 and 4). Phosphorylation of IRAK1/4 promotes phosphorylation of TRAF6 (tumor necrosis factor receptor-associated factor 6) and initiates a signaling cascade that overlaps with tumor necrosis factor (TNF) receptor signaling. This signaling cascade activates multiple transcription factors, including NF- κ B (Nuclear factor kappa-light-chain-enhancer of activated B cells (NF- κ B) and AP-1 (activator protein 1). **B.** IL-1 receptor 2 (IL-1R2) is a non-signaling decoy receptor for IL-1 lacking TIR domains. IL-R2 has 100-fold greater binding affinity for IL-1 β over IL-1 α . The *Il1r2* gene encodes both a membrane-bound and soluble (*sIl1r2*) splice variant. **C.** Membrane-bound IL-1R2 binds and serves as a sink for both IL-1 β and IL-1RAP. The heterodimer between IL-1R2 and IL-1RAP does not signal. Membrane-bound IL-1R2 can be cleaved by matrix metalloproteases to form soluble *sIL-1R2*. **D.** IL-1 receptor antagonist (IL-1RA or IL-1RN) is a competitive inhibitor of IL-1R1. The receptor antagonist causes IL-1R1 to undergo a conformational change, preventing formation of a signaling heterodimer with IL-1RAP.

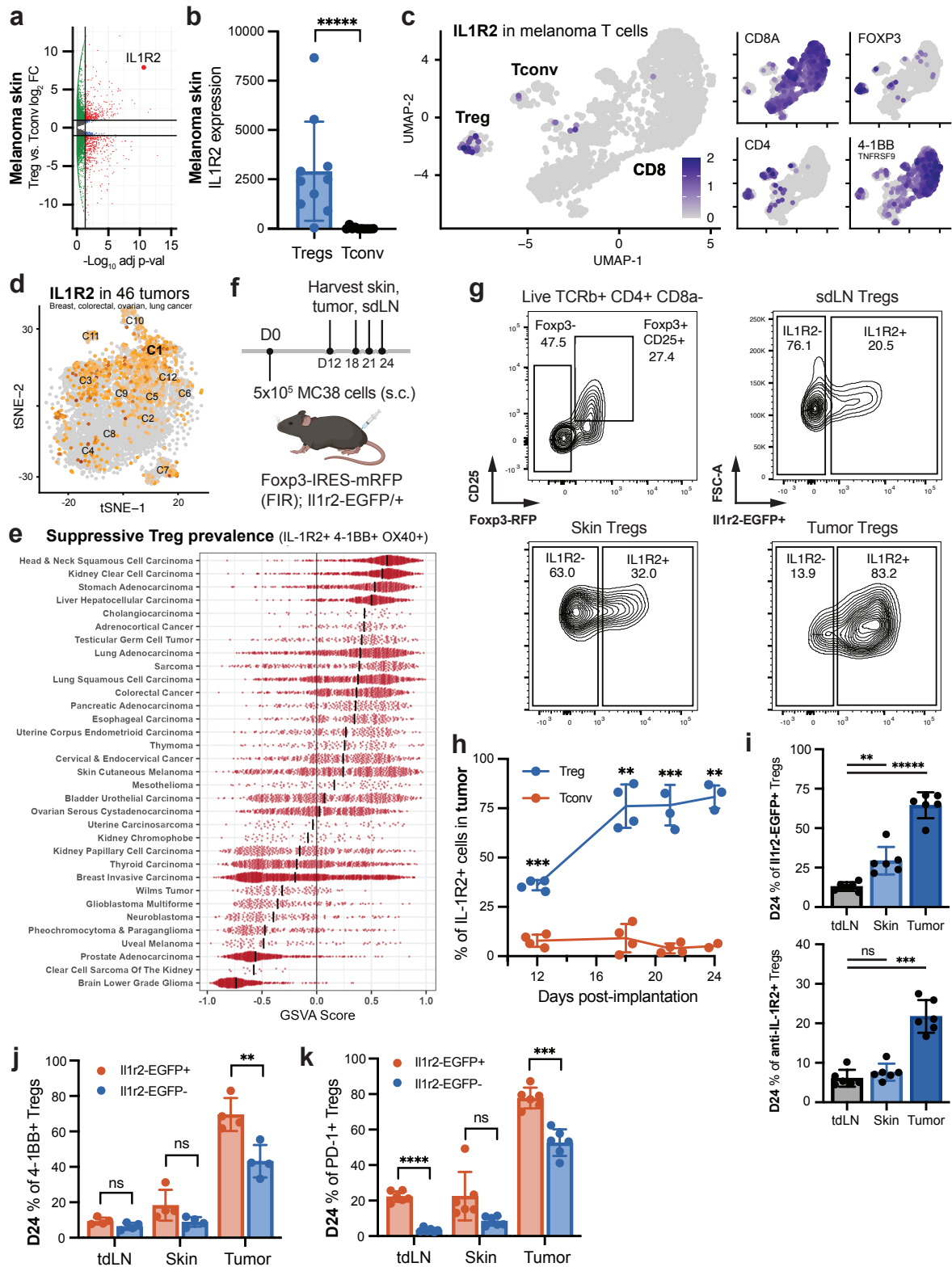


Figure 2.2 Suppressive Tregs highly express IL-1R2 in human tumors

A. Volcano plot of gene expression in regulatory T cells (Treg) vs. conventional CD4⁺ T cells (Tconv) from melanoma skin by bulk RNA sequencing (RNAseq). Data reanalyzed from Mahuron et al. (2020). IL1R2 expression is highlighted. **B.** IL1R2 counts in Tregs vs. Tconv cells from melanoma skin by bulk RNAseq. **C.** Uniform manifold approximation and projection (UMAP) plot of T cell IL1R2 expression from a melanoma sample by single-cell RNAseq (scRNAseq). **Inset:** UMAP plots of CD8A, FOXP3, TNFRSF9 (4-1BB, CD137), and CD4 expression (clockwise). **D.** T-distributed stochastic neighbor embedding (t-SNE) plot with IL1R2 expression on Tregs from 46 human tumors (breast, colorectal, ovarian, lung) by scRNAseq, with clustering overlaid. IL1R2 expressing cluster 1 is highlighted. Data reanalyzed from Qian et al. (2020). **E.** Prevalence of suppressive Tregs across 33 different tumors types from the Cancer Genome Atlas (TCGA) by gene set variation analysis (GSVA). Suppressive Treg signature composed of IL1R2, TNFRSF9 (4-1BB), and TNFRSF4 (OX40). **F.** MC38 tumor time course using Foxp3-IRES-mRFP; Il1r2-EGFP/+ dual-reporter mice. **G.** Representative flow plots of Treg (Foxp3-RFP⁺ CD25⁺) and Tconv cell (Foxp3-RFP⁻) gating, and Il1r2-EGFP reporter expression on Tregs from skin draining lymph node (sdLN), tumor, and skin on Day 24 post-MC38 implantation (clockwise). **H.** Percent of IL-1R2⁺ cells among tumor Tregs vs. Tconv cells over time. **I.** Comparison of IL-1R2 expression using an Il1r2-EGFP/+ reporter (**left**) or anti-IL-1R2 antibody clone 4E2 (**right**). Tregs from tumor draining lymph nodes (tdLN) (CD25^{hi} CD127⁻), skin or tumor (CD25⁺ ICOS⁺) of Il1r2-EGFP/+ reporter mice on Day 24 post-MC38 implantation. Expression of 4-1BB (**J**) and PD-1 (**K**) on Il1r2-EGFP⁺ vs. Il1r2-EGFP⁻ Tregs from tdLN, skin, and tumor of mice on Day 24 post-MC38 implantation. Results are shown as mean \pm SD, with dots representing individual patients or mice (**B**, **H-K**). Statistics are calculated using unpaired (**B**, **I**) or paired two-tailed t-tests (**H**, **J**, **K**) with a False Discovery Approach (FDR) for multiple comparisons (Benjamini). *, $p < 0.05$; **, $p < 0.01$; ***, $p < 0.001$; ****, $p < 0.0001$; *****, $p < 0.00001$; ns, not significant. FC, fold change. Adj p-val, adjusted p-value. s.c., subcutaneous. FSC-A, forward scatter area.

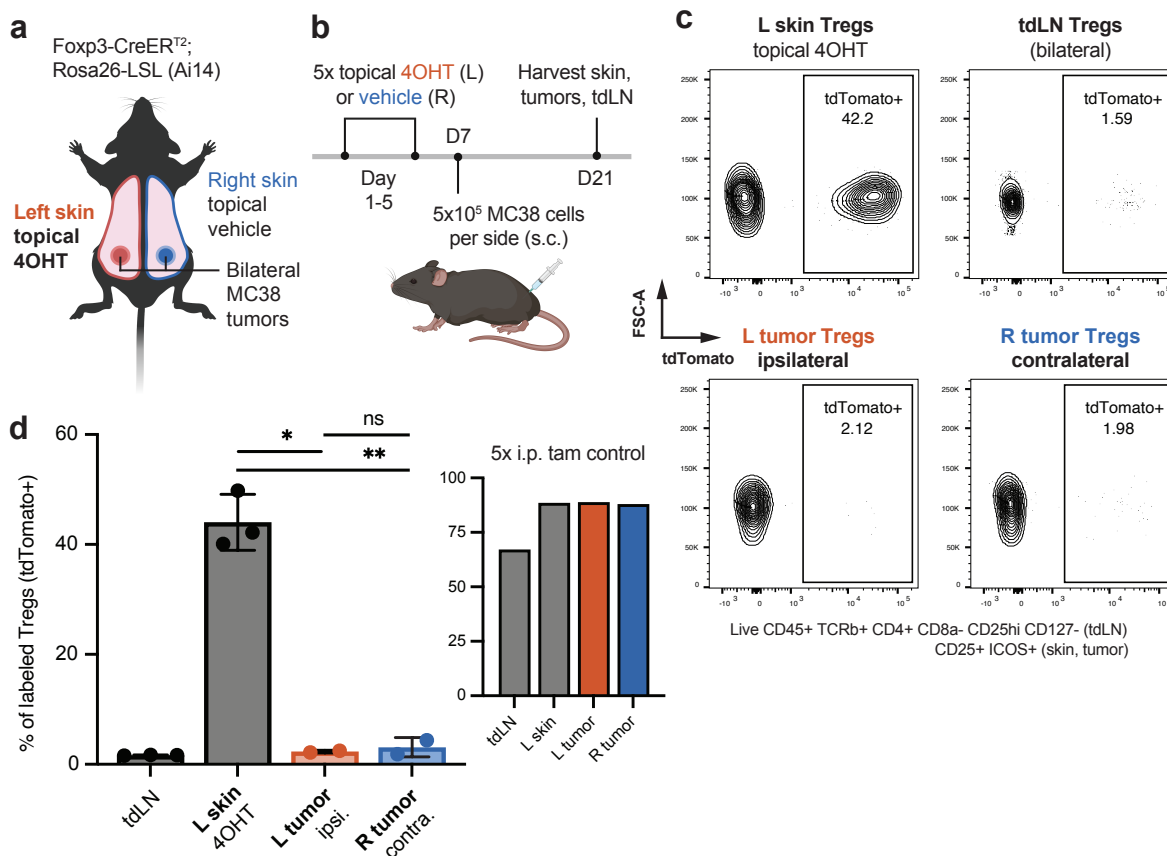


Figure 2.3 IL-R2+ tumor Tregs are not predominantly derived from adjacent skin

A. Diagram of topical z-4-hydroxytamoxifen (4OHT) and vehicle (acetone) application on left and right back skin, respectively. **B.** Foxp3-CreER^{T2}; Rosa26-LSL (Ai14) mice were treated with 4OHT and vehicle for 5 days, followed by s.c. MC38 injection into left and right flanks. **C.** Representative flow plots of tdTomato expression on Tregs from left skin (topical 4OHT-treated), tdLN (bilateral), right tumor (contralateral to 4OHT), and left tumor (ipsilateral to 4OHT) on Day 21 (clockwise). Tregs were gated on CD25hi CD127- (tdLN) or CD25+ ICOS+ (skin, tumor). **D.** Percent of tdTomato labeled Tregs per tissue on Day 21 after topical 4OHT. **Inset:** Percent of tdTomato labeled Tregs in a control mouse treated with 5 days of intraperitoneal (i.p.) tamoxifen (tam). Results are shown as mean \pm SD, with dots representing individual mice (**D**). Statistics are calculated using paired two-tailed t-tests with a False Discovery Approach (FDR) for multiple comparisons (Benjamini). *, $p < 0.05$; **, $p < 0.01$; ns, not significant.

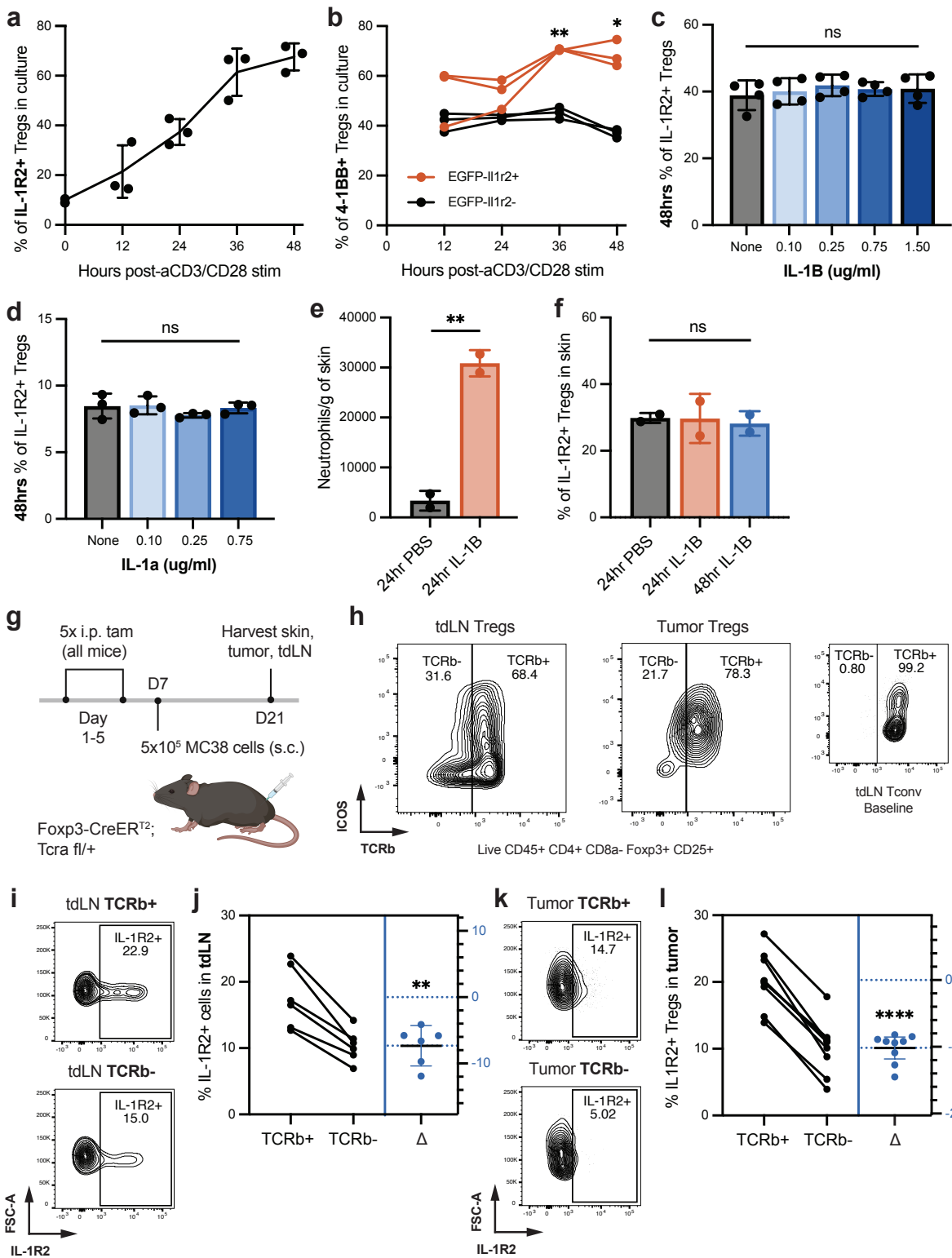


Figure 2.4 Tumor Tregs upregulate IL-1R2 in response to TCR stimulation but not IL-1 family members

A. Percent of Il1r2-EGFP expression on mouse Tregs in culture. Tregs were sorted from sdLN and spleen of dual-reporter mice, then cultured with anti-CD3/anti-CD28 (α CD3/CD28) beads at a 3:1 bead:cell ratio. **B.** Expression of 4-1BB on Il1r2-EGFP+ vs. Il1r2-EGFP- Tregs in culture. **C.** Expression of IL-1R2 on Tregs (CD4+ Foxp3-RFP+) after 48 hours in culture with mixed lymphocytes and varying concentrations of IL-1 β . **D.** Expression of IL-1R2 on sorted Tregs after 48 hours in culture with suboptimal α CD3/CD28 activation at a 1:10 bead:cell ratio and varying concentrations of IL-1 α . **E.** Neutrophils per gram skin following s.c. injection of 200 ng IL-1 β or PBS. Neutrophil influx used to confirm IL-1 β -mediated inflammation. **F.** Percent of Il1r2-EGFP expressing skin Tregs following s.c. injection of IL-1 β or PBS. **G.** Foxp3-CreER^{T2}; Tcra-fl/+ were treated with i.p. tamoxifen for 5 days, followed by MC38 injection in the left flank. **H.** Representative flow plots of TCR β expression on tdLN (left) and tumor (right) Tregs on Day 21. TCR β staining used as a proxy for TCR α presence. **I.** Representative flow plots and quantification (**J**) of IL-1R2 expression on TCR β + vs. TCR β - Tregs in tdLN using anti-IL-1R2 antibody staining. **K.** Representative flow plots and quantification (**L**) of IL-1R2 expression on TCR β + vs. TCR β - Tregs in tumors using antibody. Results are shown as mean \pm SD, with dots representing individual mice. Statistics are calculated using one way ANOVA (**A-D**) and paired two-tailed t-tests (**B, E, F, J, L**) with a False Discovery Approach (FDR) for multiple comparisons (Benjamini). *, $p < 0.05$; **, $p < 0.01$; ****, $p < 0.0001$; ns, not significant.

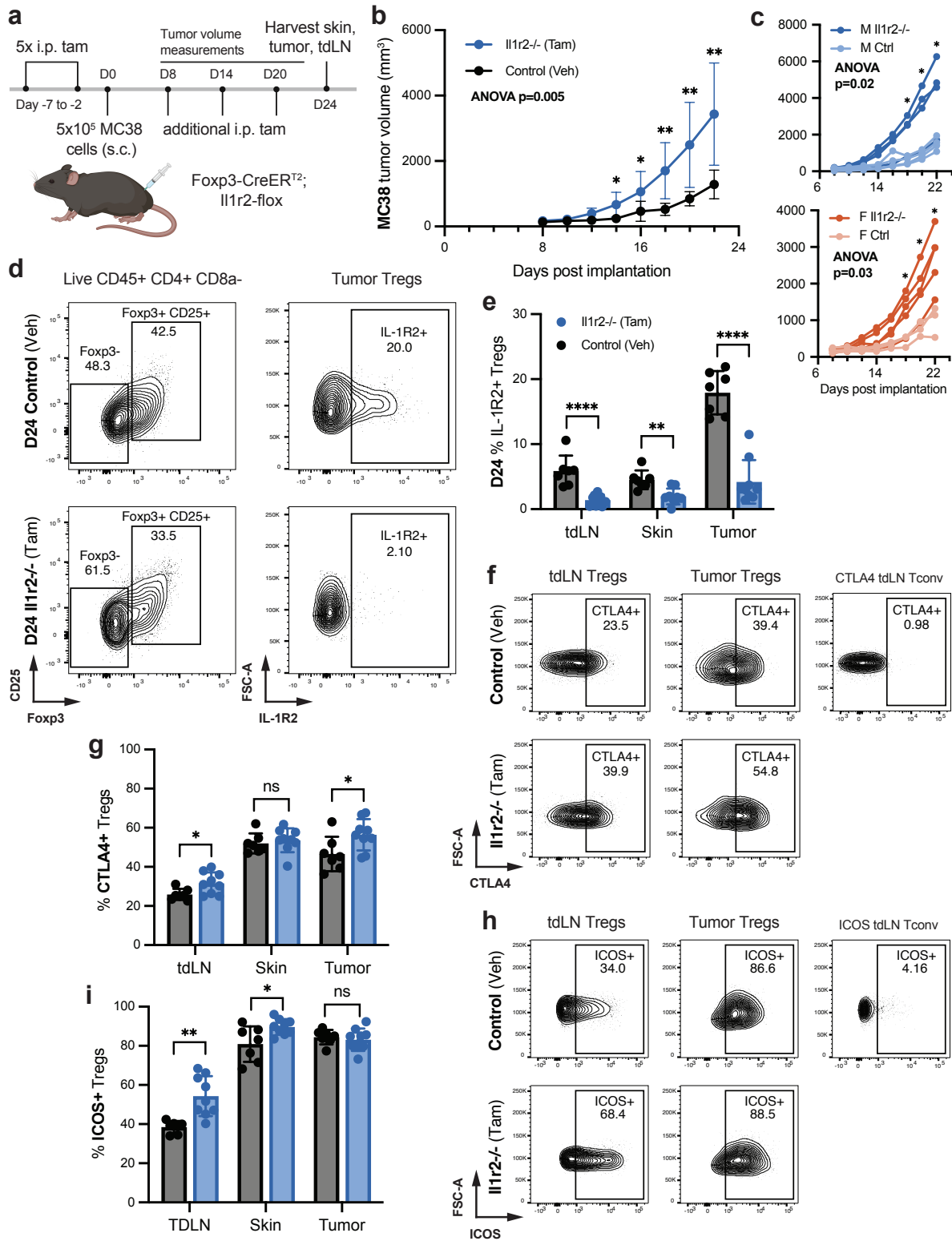


Figure 2.5 IL-1R2 expression on Tregs results in reduced tumor growth *in vivo*

A. Foxp3-CreER^{T2}; Il1r2-Flox mice were treated with i.p. tamoxifen (tam) or vehicle (corn oil) for 5 days, followed by MC38 injection in the left flank. Tumor volume ($w \times h \times [w+h] \times 0.5$) was measured from Day 8-22. **B.** MC38 tumor volume on tam-treated Il1r2^{-/-} mice vs. vehicle-treated (veh) control mice over time. **C.** Tumor volume data divided into male (left) and female (right) mice. **D.** Representative flow plots of Treg (Foxp3⁺ CD25⁺) and Tconv cell (Foxp3⁻) gating in tumor (left). IL-1R2 expression on tumor Tregs using anti-IL-1R2 antibody staining (right). **E.** Percent of IL-1R2⁺ Tregs in Il1r2^{-/-} vs. control mice, grouped by tissue. **F.** Representative flow plots and quantification (**G**) of CTLA4 expression on Il1r2^{-/-} vs. control Tregs, grouped by tissue. Baseline CTLA4 expression set in Tconv cells from tdLN. **H.** Representative flow plots and quantification (**I**) of ICOS expression on Il1r2^{-/-} vs. control Tregs, grouped by tissue. Baseline ICOS expression set in Tconv cells from tdLN. Results are shown as mean \pm SD, with dots representing individual mice. Statistics are calculated using one way ANOVA (**B, C**) and unpaired two-tailed t-tests (**B, C, E, F, H, J**) with a False Discovery Approach (FDR) for multiple comparisons (Benjamini). *, $p < 0.05$; **, $p < 0.01$; ****, $p < 0.0001$; ns, not significant.

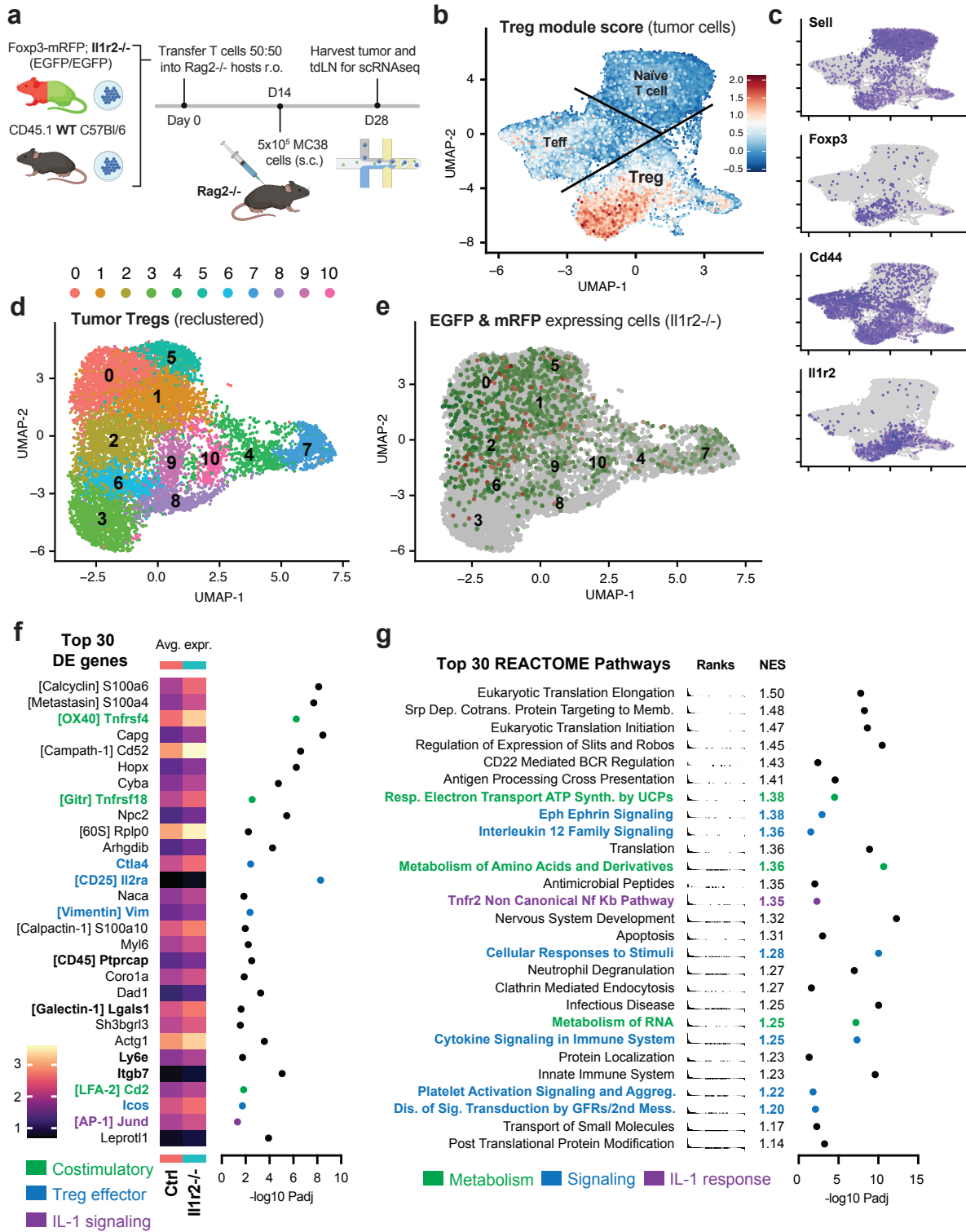


Figure 2.6 IL-1R2 attenuates Treg activation in tumors

A. T cells from Foxp3-IRES-mRFP; Il1r2-EGFP/EGFP mice (Il1r2^{-/-}) and CD45.1 C57Bl/6 mice (Ctrl) were transferred at a 50:50 ratio into Rag2^{-/-} hosts via retro-orbital (r.o.) injection. Rag2^{-/-} hosts were injected with MC38 on Day 14. CD4⁺ T cells from tumor and tdLN were collected for scRNAseq on Day 28. **B.** UMAP plot of CD4⁺ T cells from MC38 tumor with Treg module score and cell identities overlaid. **C.** UMAP plots of Sell (L-selectin, CD62L), Cd44, Il1r2, and Foxp3 (descending). **D.** UMAP of tumor Tregs after subsetting and reclustering. Cells are colored and labeled by cluster. **E.** UMAP of tumor Tregs with expression of EGFP (green) and mRFP (red) overlaid. **F.** Top 30 differentially expressed (DE) genes enriched in Il1r2^{-/-} tumor Tregs vs. Ctrl Tregs by fold change. **Left:** gene names, labeled by category. **Middle:** heatmap of average gene expression in Il1r2^{-/-} vs. Ctrl cells. **Right:** -log₁₀ adjusted P-value of DE genes. **G.** Top significantly enriched REACTOME pathways in Il1r2^{-/-} vs. Ctrl Tregs using gene set enrichment analysis (GSEA). **Left:** pathway names, labeled by category. **Middle:** gene rank plots and normalized enrichment scores (NES) of each pathway. **Right:** -log₁₀ adjusted P-value of REACTOME pathways.

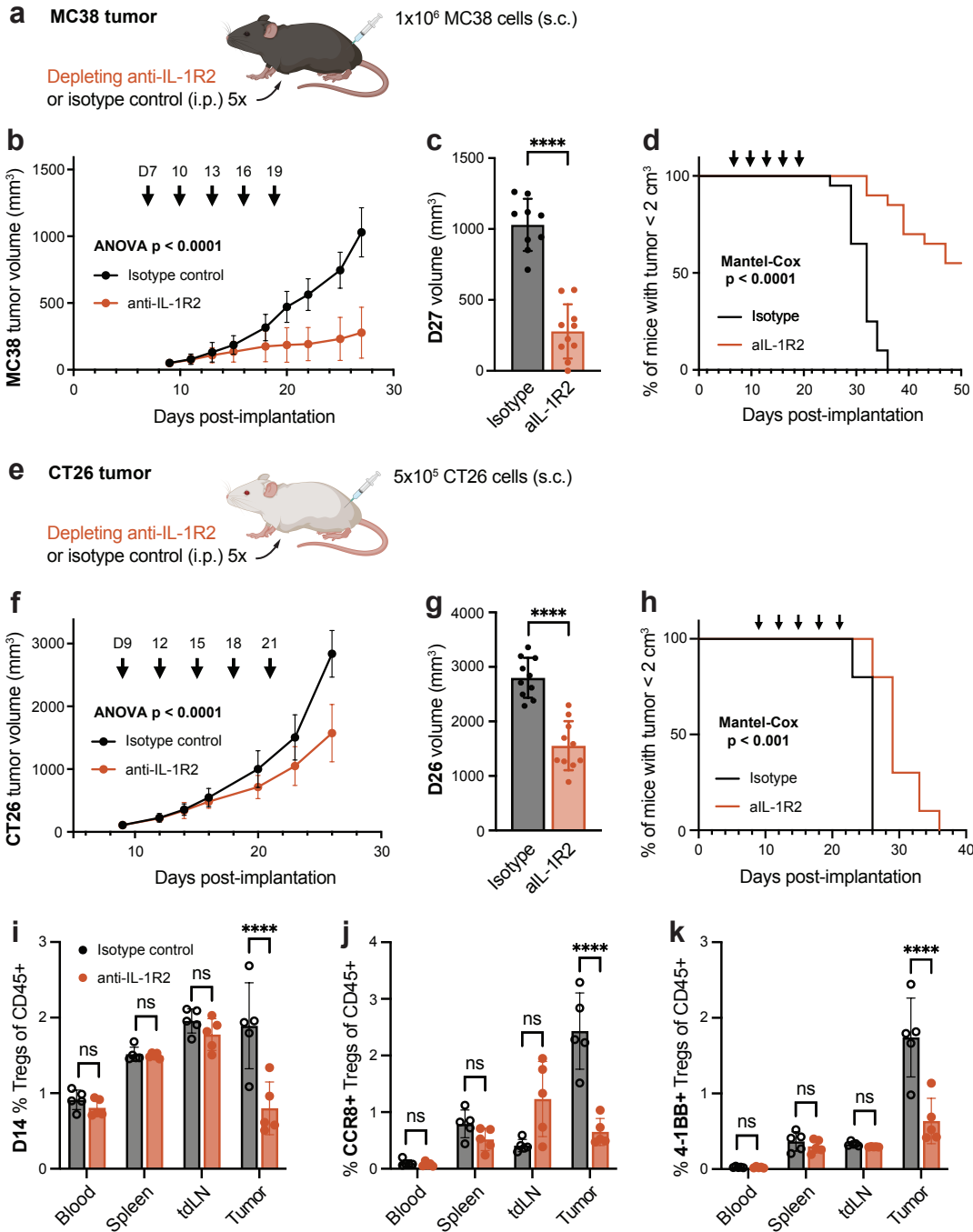


Figure 2.7 Depleting IL-1R2 expressing Tregs reduces tumor growth

A. C57Bl/6 mice were injected with MC38 cells and treated with 5 x 600 μ g of depleting anti-IL-1R2 antibody (aIL-1R2) vs. IgG2A isotype control on Day 7, 10, 13, 16, and 19 post-implantation (arrows). **B.** MC38 tumor volume in mice treated with aIL-1R2 vs. isotype over time. **C.** MC38 tumor volume at Day 27 post-implantation. **D.** Survival curve of MC38 tumor-bearing mice until experimental endpoint (tumor volume > 2 cm³). **E.** Balb/C mice were injected with CT26 cells and treated with 5 days of depleting aIL-1R2 vs. isotype control on Day 9, 12,

15, 18, and 21 post-implantation. **F.** CT26 tumor volume in mice treated with aIL-1R2 vs. isotype over time. **G.** CT26 tumor volume on Day 26 post-implantation. **H.** Survival curve of CT26 tumor-bearing mice until experimental endpoint (tumor volume > 2 cm³). **I.** Percent of Tregs (Foxp3+ CD25+) among total CD45+ cells in aIL-1R2 vs. isotype treated mice by flow cytometry. Cells isolated from blood, spleen, tdLN, and tumor on Day 14 post-CT26 implantation. **J.** Percent of CCR8+ Tregs and 4-1BB+ Tregs (**K.**) among total CD45+ cells by flow cytometry. Cells isolated on Day 14 post-CT26 implantation, grouped by treatment and tissue. Results are shown as mean +/- SD, with dots representing individual mice. Statistics are calculated using one way ANOVA (**B, F**), Mantel-Cox log-rank test (**D, H**) and unpaired two-tailed t-tests (**C, G, I-K**) with a False Discovery Approach (FDR) for multiple comparisons (Benjamini). ****, $p < 0.0001$; ns, not significant.

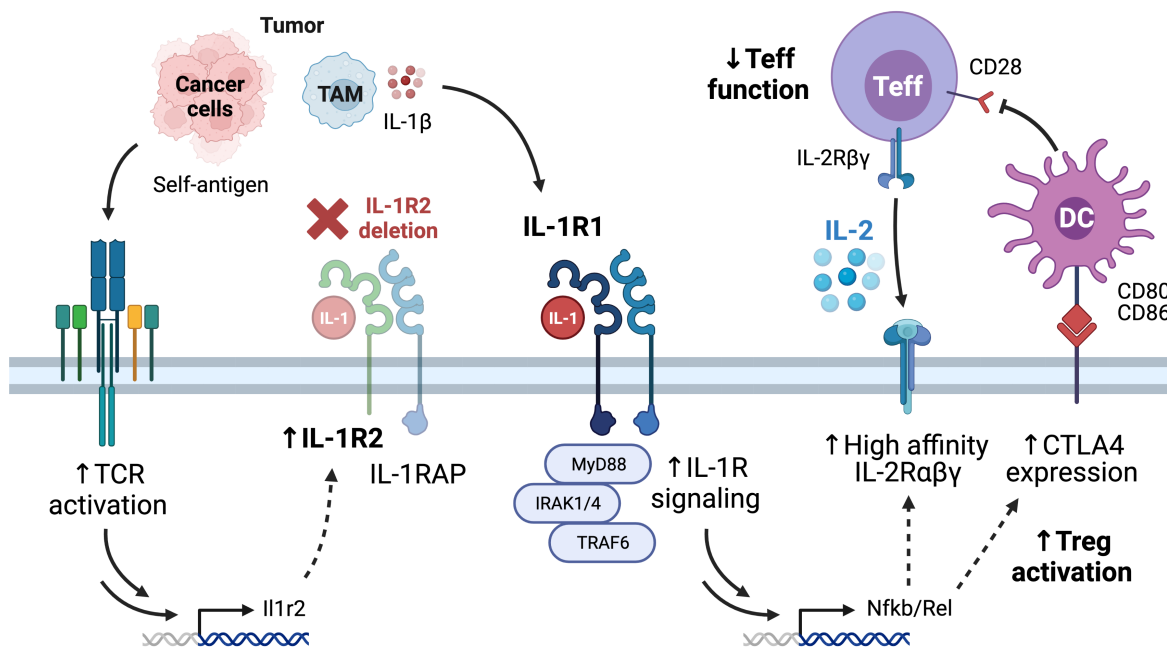


Figure 2.8 Model of IL-1R2 function on tumor Tregs

Cancer cells generate self-antigens, which engage the T cell receptor (TCR) on tumor-associated Tregs. TCR engagement promotes IL-1R2 expression on tumor Tregs. Tregs use membrane-bound IL-1R2 to limit IL-1R signaling in a cell-intrinsic fashion. Tumor-associated macrophages (TAMs) and other activated myeloid cells produce IL-1 β in the tumor. Deletion of IL-1R2 on Tregs leads to increased IL-1R1 signaling and expression of transcription factor NF- κ B (Nfkb1/2, Rela/b, Rel). NF- κ B increases expression of Treg effector genes, including *Il2ra* and *Ctla4*. High affinity IL-2R $\alpha\beta\gamma$ reduces free IL-2 available for CD8+ and CD4+ Teff cells. CTLA4 binds and endocytoses CD80/CD86 on APCs, preventing Teff binding through CD28. Together, IL-1 signaling increases Treg activation to suppress Teff function in the tumor.

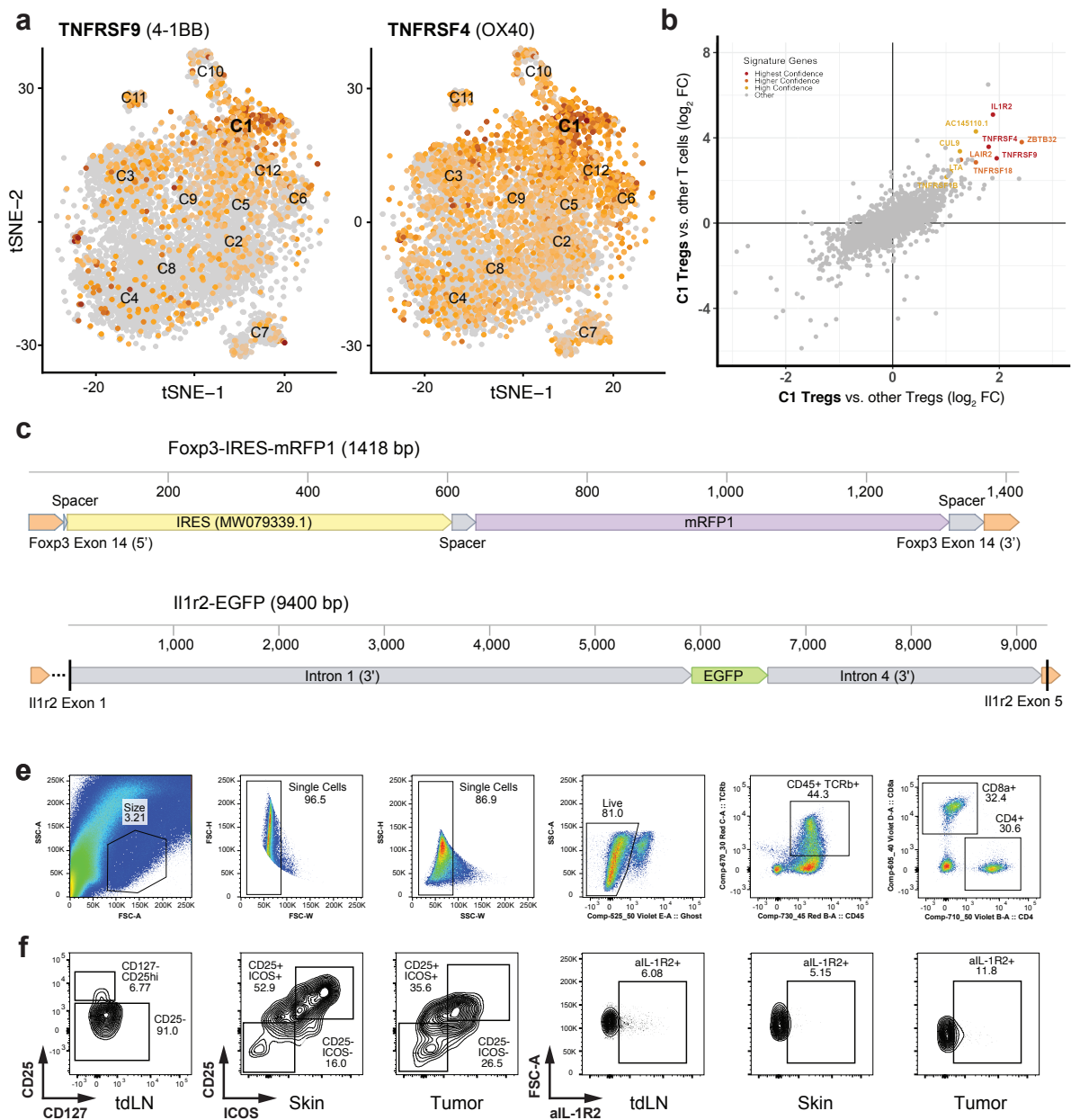


Figure 2.9 Supplement to suppressive Tregs highly express IL-1R2 in human tumors

A. t-SNE plots of TNFRSF9 (4-1BB) expression (left) and TNFRSF4 (OX40) expression (right) on Tregs from 46 human tumors (breast, colorectal, ovarian, lung) by scRNAseq, with d clustering overlaid. Suppressive cluster 1 is highlighted. Data reanalyzed from Qian et al. (2020).

B. Scatter plot of gene expression in cluster 1 Tregs vs. other Tregs (x-axis) and vs. other T cells (y-axis) by \log_2 FC. Most significantly enriched genes are labeled in the upper right corner and colored by p-value and \log_2 FC to define a gene signature for suppressive cluster 1. Signature genes included IL1R2, TNFRSF9, TNFRSF4, TNFRSF18 (GITR), LAIR2 (Leukocyte-associated Ig-like receptor 2), ZBTB32 (Zinc finger and BTB domain containing 32), LTA (lymphotoxin A), CUL9 (Cullin 9), and TNFRSF1B (TNF receptor 2). Highest confidence required x-axis: $p < 1 \times 10^{-30}$ and \log_2 FC > 1.5 , y-axis: $p < 1 \times 10^{-50}$ and \log_2 FC > 3 , z-axis $p <$

1×10^{-75} and $\log_2 \text{FC} > 4$ (not shown, C1 Tregs vs. all other tumor cells). **C.** Diagram of Foxp3 in Foxp3-IRES-mRFP (FIR) mice: IRES-mRFP1 construct inserted into the untranslated portion of exon 14 (top). Diagram of Il1r2 in Il1r2-EGFP reporter mice: EGFP replaces exons 2-4 to inhibit Il1r2 translation (bottom). **D.** Flow gating strategy for CD4⁺ T cells from MC38 tumors. **E.** From left to right: flow gating strategy for surface labeling of Tregs in tdLN using surrogate markers CD25^{hi} CD127⁻ (panel 1), in skin using CD25⁺ ICOS⁺ (p2), and tumor using CD25⁺ ICOS⁺ (p3). Representative flow plots of anti-IL-1R2 antibody staining on Tregs from tdLN (p4), skin (p5), and tumor (p6). For simultaneous staining with the Il1r2 reporter and antibody, cells could not be permeabilized to preserve Il1r2-EGFP signal, and Foxp3-RFP could not be used due to overlap with phycoerythrin (PE) anti-IL-1R2.

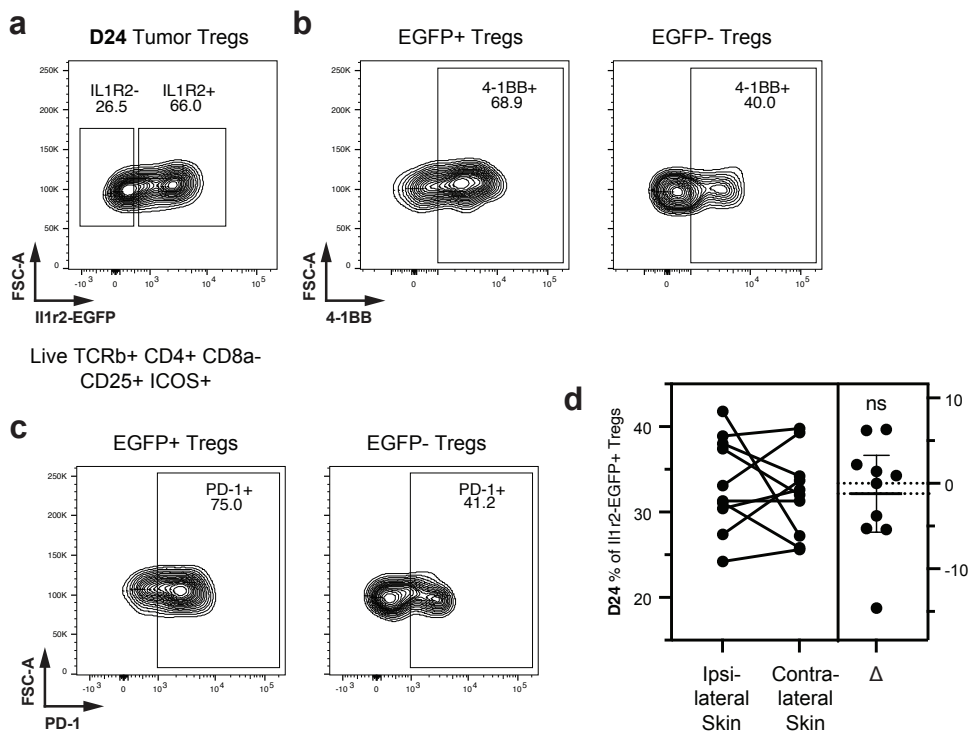


Figure 2.10 Il1r2-EGFP expression in tumor and skin of MC38-bearing mice

A. Representative flow plot of Il1r2-EGFP expression on tumor Tregs 24 days post-MC38 implantation. **B.** Representative flow plots of 4-1BB expression on EGFP⁺ (left) and EGFP⁻ Tregs (right) from the same mouse on Day 24. **C.** Representative flow plots of PD-1 expression on EGFP⁺ (left) and EGFP⁻ Tregs (right) from the same mouse on Day 24. **D.** Il1r2-EGFP reporter expression on Tregs from back skin adjacent to implanted MC38 tumor (ipsilateral) or on the opposite side (contralateral). Each pair of dots represents a mouse. Statistics are calculated using a paired two-tailed t-test. ns, not significant.

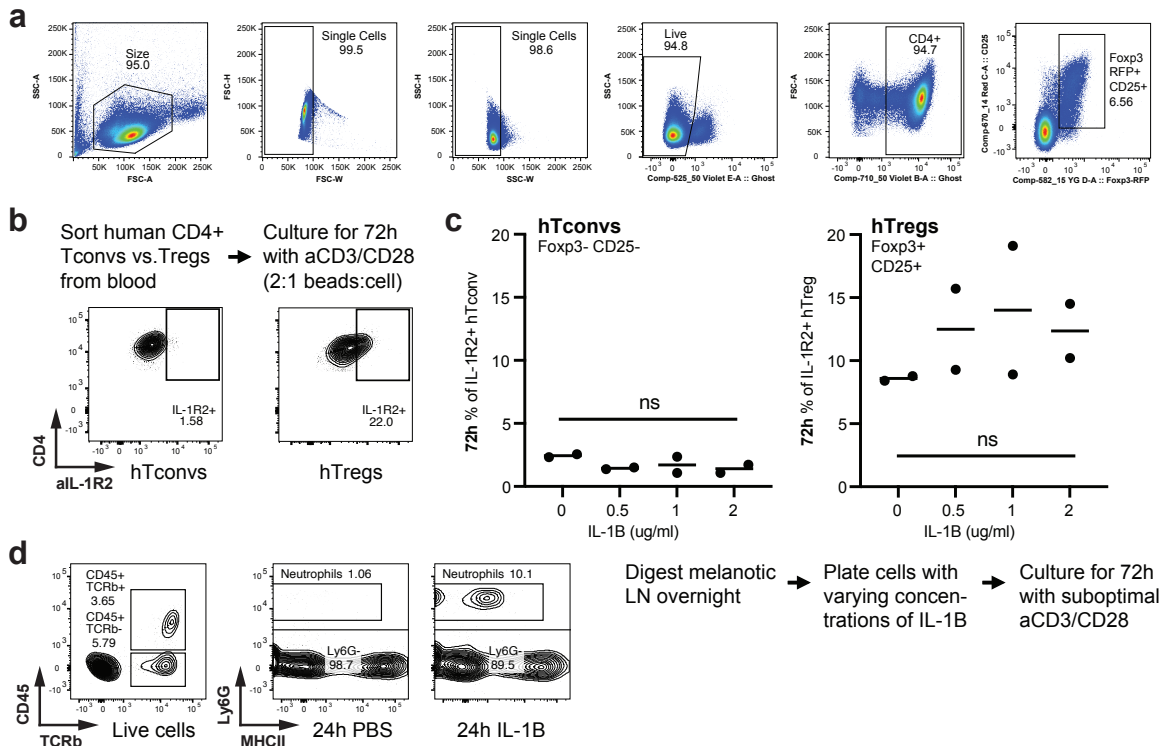


Figure 2.11 Supplement to tumor Tregs upregulate IL-1R2 in response to TCR stimulation but not IL-1 family members

A. Fluorescence activated cell sorting (FACS) strategy for Tregs from Foxp3-RFP; Il1r2-EGFP dual reporter mice. **B.** IL-1R2 expression on human CD4⁺ T conventional cells (hTconv) and human Tregs (hTreg) *in vitro* using anti-IL-1R2 clone 34141. Cells were isolated from human blood, sorted on Live TCRβ⁺ CD4⁺ CD25⁻ (hTconv) or CD4⁺ CD25^{hi} CD127⁻ (hTreg), and cultured for 72 hours with αCD3/CD28 beads. **C.** IL-1R2 expression on hTconv and hTreg from melanotic LN with IL-1β. Two melanotic LN were digested overnight, then plated with varying concentrations of IL-1β, and cultured for 72 hours with suboptimal 0.1 μg/ml αCD3/CD28. Statistics are calculated using paired two-tailed t-tests. ns, not significant. **D.** From left to right: representative flow plots of myeloid cell gating in control mouse skin (24h PBS) (panel 1); neutrophil staining in skin 24 hours after s.c. injection with PBS (p2) or IL-1β (p3).

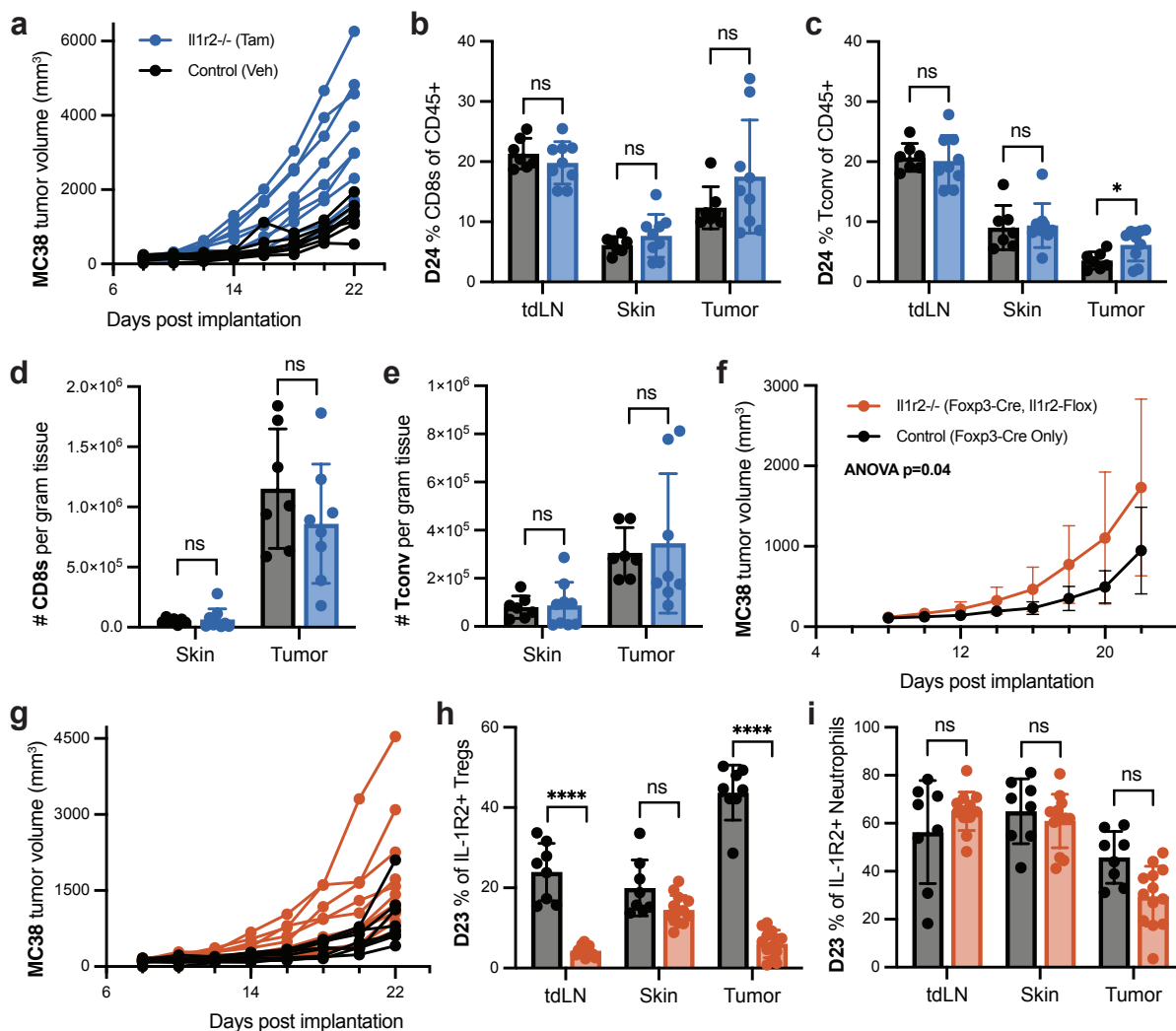


Figure 2.12 Supplement to IL-1R2 expression on Tregs results in reduced tumor growth *in vivo*

A. Individual MC38 tumor growth curves for Foxp3-CreERT2; Il1r2-Flox mice treated with tam (Il1r2^{-/-}) or veh (Control). **B.** Percent of CD8⁺ T cells out of total CD45⁺ cells in tdLN, skin, and tumor on Day 24 post-MC38 implantation, grouped by treatment. **C.** Percent of CD4⁺ Tconv cells out of total CD45⁺ cells on Day 24, grouped by treatment. Absolute number of CD8⁺ cells (**D**) and Tconv cells (**E**) per gram of skin or tumor on Day 24, grouped by treatment. **F.** MC38 tumor volume on Foxp3-Cre; Il1r2-Flox mice (Il1r2^{-/-}) vs. Foxp3-Cre only mice (Control) over time. **G.** Individual MC38 tumor growth curves for Il1r2^{-/-} vs. Control mice. **H.** Percent of anti-IL-1R2 antibody expression on Tregs in tdLN, skin, and tumor on Day 23 post-MC38 implantation, grouped by genotype. **I.** Percent of IL-1R2 expression on neutrophils on Day 23 suggests that Foxp3-Cre is Treg specific. Note that neutrophils are infrequent in tdLN, skin, and tumor. Statistics are calculated using one-way ANOVA (**F**) or unpaired two-tailed t-tests (**B**, **C**, **D**, **E**, **H**, **I**) with a False Discovery Approach (FDR) for multiple comparisons (Benjamini). *, p < 0.05; ****, p < 0.0001; ns, not significant.

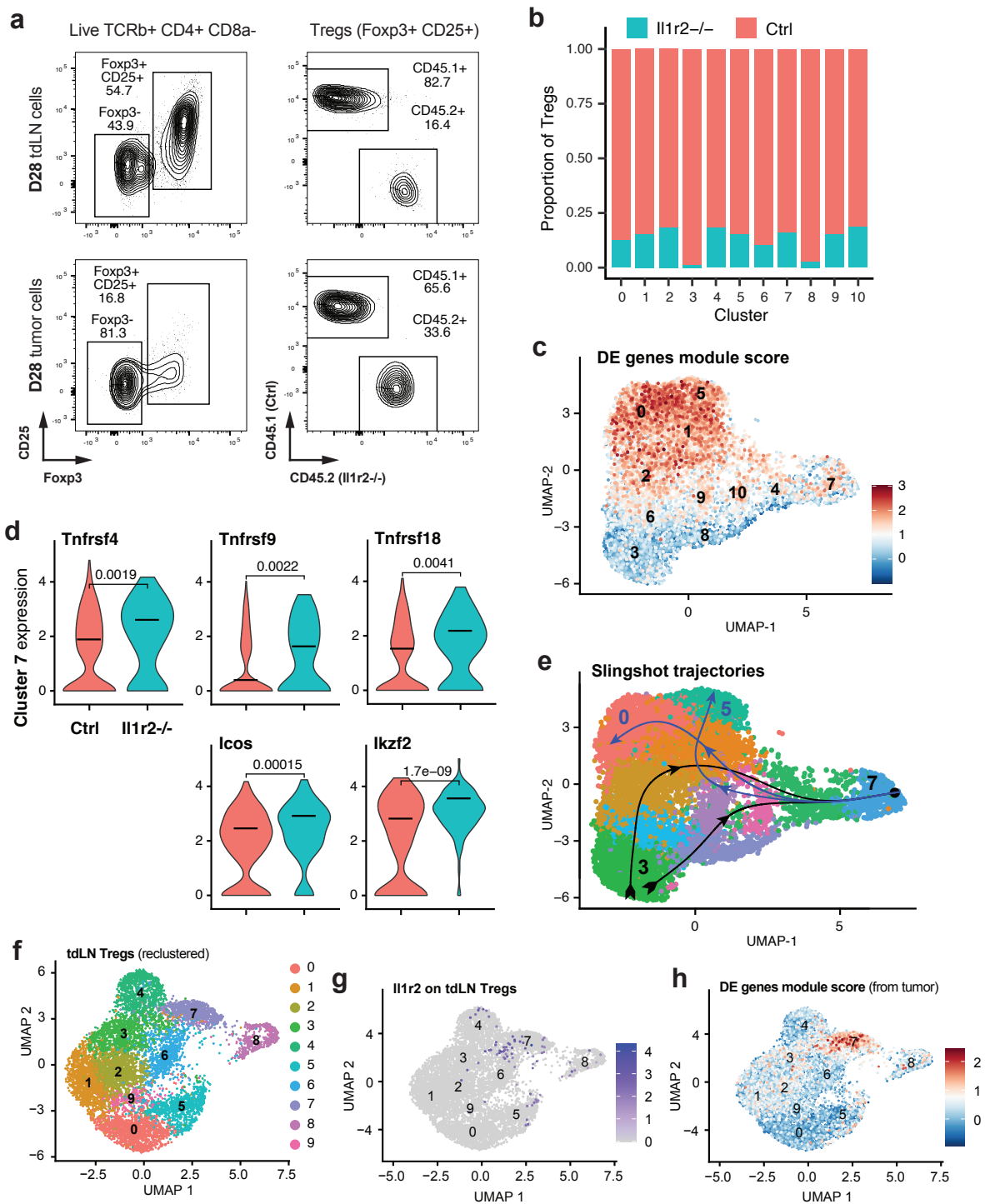


Figure 2.13 Supplement to IL-1R2 attenuates Treg activation in tumors

A. Percent of Tregs among CD4+ T cells (left) and ratio of CD45.1+ (Ctrl) to CD45.2+ (Il1r2-/-) Tregs (right) in a Rag2^{-/-} host 28 days after cell transfer. tdLN (top) and tumor (bottom) harvested for flow analysis before proceeding with scRNAseq experiment. **B.** Fraction of Il1r2^{-/-} tumor Tregs (EGFP and/or mRFP expressing) vs. Ctrl Tregs per cluster. **C.** UMAP of tumor

Tregs with module score composed of top DE genes from Figure 2.5F. **D.** Violin plots of *Tnfrsf4* (OX40), *Tnfrsf9* (4-1BB), *Tnfrsf18* (GITR), *Icos*, and *Ikzf2* (Helios) gene expression among Tregs in cluster 7, divided by treatment. Median expression and p-value of unpaired two-tailed t-tests overlaid. **E.** Branching lineage structure (developmental trajectory) analysis using Slingshot. Cluster 3 on control cells (low activation) set as starting point, with two independent trajectories moving toward cluster 7 (intermediate activation), then ending at cluster 0 or cluster 5 (high activation). **F.** scRNAseq of tdLN from *Rag2*^{-/-} mice with transferred CD45.1 WT and CD45.2 *Il1r2*^{-/-} T cells. UMAP of tdLN Tregs after subsetting and clustering. Cells are colored and labeled by cluster. **G.** UMAP of *Il1r2* expression on tdLN Tregs. **H.** UMAP of tdLN Tregs with module score of top DE genes from *Il1r2*^{-/-} tumor Tregs, as in Figure 2.11C.

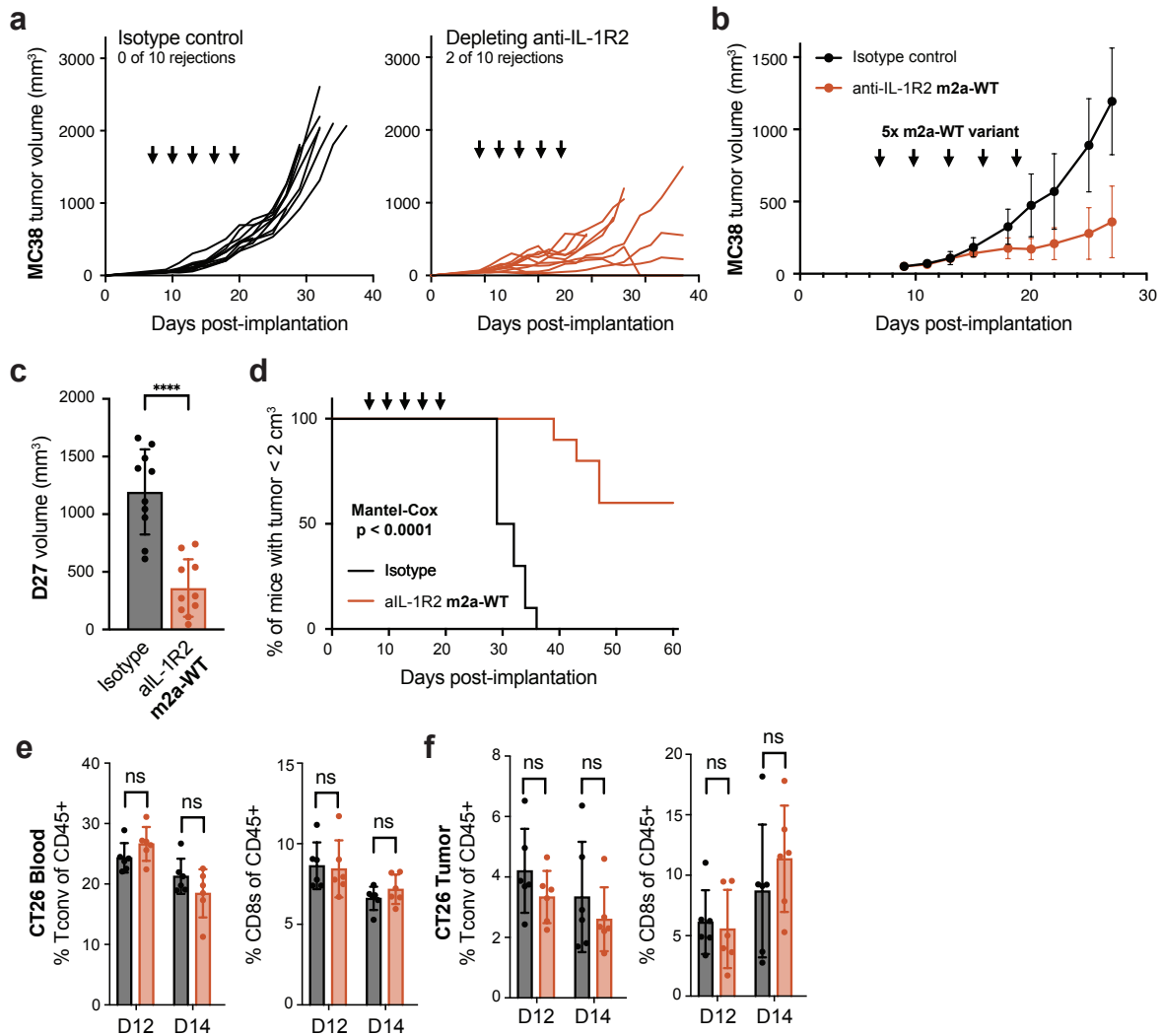


Figure 2.14 Supplement to depleting IL-1R2 expressing Tregs reduces tumor growth
A. Individual MC38 tumor growth curves C57Bl/6 mice treated with 5 x 600 µg of IgG2A isotype control (left) or depleting anti-IL-1R2 antibody (right). Tumor rejection observed in 0 of 10 control mice vs. 2 of 10 anti-IL-1R2 treated mice. **B.** Percent of CD4⁺ Tconv cells (left) and CD8⁺ cells (right) out of total CD45⁺ cells in the blood of Balb/C mice on Day 12 and 14

post-CT26 implantation, grouped by treatment. **C.** Percent of CD4⁺ Tconv cells (left) and CD8⁺ cells (right) out of total CD45⁺ cells in CT26 tumor on Day 12 and 14, grouped by treatment. Results are shown as mean \pm SD, with dots representing individual mice. Statistics are calculated using unpaired two-tailed t-tests (**B, C**) with a False Discovery Approach (FDR) for multiple comparisons (Benjamini). ns, not significant.

Publishing Agreement

It is the policy of the University to encourage open access and broad distribution of all theses, dissertations, and manuscripts. The Graduate Division will facilitate the distribution of UCSF theses, dissertations, and manuscripts to the UCSF Library for open access and distribution. UCSF will make such theses, dissertations, and manuscripts accessible to the public and will take reasonable steps to preserve these works in perpetuity.

I hereby grant the non-exclusive, perpetual right to The Regents of the University of California to reproduce, publicly display, distribute, preserve, and publish copies of my thesis, dissertation, or manuscript in any form or media, now existing or later derived, including access online for teaching, research, and public service purposes.

DocuSigned by:

Ireneusz Habrylo

D581949403F2419...

Author Signature

3/9/2023

Date